

# Semi-supervised Vector-valued Learning: From Theory to Algorithm

Jian Li\*, Yong Liu\*<sup>†</sup>, and Weiping Wang.

## Abstract

Vector-valued learning, where the output space admits a vector-valued structure, is an important problem that covers a broad family of important domains, e.g. multi-label learning and multi-class classification. Using local Rademacher complexity and unlabeled data, we derive novel data-dependent excess risk bounds for learning vector-valued functions in both the kernel space and linear space. The derived bounds are much sharper than existing ones, where convergence rates are improved from  $\mathcal{O}(1/\sqrt{n})$  to  $\mathcal{O}(1/\sqrt{n+u})$ , and  $\mathcal{O}(1/n)$  in special cases. Motivated by our theoretical analysis, we propose a unified framework for learning vector-valued functions, incorporating both local Rademacher complexity and Laplacian regularization. Empirical results on a wide number of benchmark datasets show that the proposed algorithm significantly outperforms baseline methods, which coincides with our theoretical findings.

## Index Terms

Vector-valued Functions, Semi-supervised Learning, Generalization Analysis, Local Rademacher Complexity.



## 1 INTRODUCTION

Learning vector-valued functions involves learning a predictive model from training data that has vector-valued rather than scalar-valued labels. This encompasses a wide range of important tasks, such as multi-class classification [1], [2], multi-label learning [3], [4], multi-task learning [5], [6], and so on. In this paper, we focus on the general vector-valued learning and two special cases: multi-class classification and multi-label learning.

On the algorithmic front, various models have been developed to address special cases of vector-valued learning, with a particular focus on multi-class classification and multi-label learning. For multi-class classification, approaches include maximum margin based kernel methods [1], [7], deep neural networks [8], entropy-based sampling [9], ensemble [10], [11], etc. Meanwhile, for multi-label learning, there are also well-studied methods, including linear estimators [12], k-nearest neighbor based approaches [13], [14], kernel-based learning [15] semi-supervised learning [16], partial multi-label learning [17], [18] and so on. For vector-valued functions which admit a reproducing kernel, [19], [20] presented an algorithm to learn the reproducing kernel Hilbert space (RKHS), and then [21] extended it to semi-supervised learning via manifold regularization. However, there remains a significant lack of unified learning frameworks for general vector-valued tasks in the output space rather than RKHS.

On the theoretical front, the statistical learning theory for vector-valued functions suggests that estimating the generalization ability of algorithms is key to understanding the factors that affect their performance and developing ways to improve them [22], [23]. The statistical learning theories for special cases of vector-valued functions (e.g. multi-class classification and multi-label learning) have, by now, been well developed [2], [4], [24]. For instance, the convergence rates of the generalization error bounds for multi-class classification and multi-label learning are  $\mathcal{O}(K/\sqrt{n})$  and  $\mathcal{O}(1/\sqrt{n})$ , respectively, where  $K$  is the size of the vector-valued output and  $n$  is the number of labeled samples. However, despite its importance, theoretical properties for vector-valued functions has been only scarcely studied. Theoretical results from recent works [25], [26], [27] on vector-valued functions employed the contraction inequality to estimate the global Rademacher complexity of the estimators, while the rates of their bounds are at best  $\mathcal{O}(1/\sqrt{n})$ .

Our previous works [28], [29], published in **NeurIPS** and **IJCAI**, provided origin ideas on the generalization analysis of multi-class classification with local Rademacher complexity. In this paper, we combine our previous works for multi-classification [28], [29] and generalize their theoretical analysis and algorithms for semi-supervised vector-valued settings. Compared to our previous works, we make the following significant improvements.

- Instead of using *generalization error bounds* for multi-class classification in the kernel space [28] or linear space [29], we derive *excess risk bounds* for vector-valued learning in both linear and kernel spaces.
- We provide a unified theoretical results for semi-supervised vector-valued learning in both kernel space and linear space, while the previous works only work for multi-class classification.
- We use a milder assumption for the loss function. Our earlier works assumed the loss function to be  $L$ -smooth, while this paper just needs  $L$ -Lipschitz continuous condition on the loss function.

• J. Li and Y. Liu contribute equally. Y. Liu is also the corresponding author. Email: lijian@ie.ac.cn, liuyonggsai@ruc.edu.cn.  
 • J. Li and W. Wang are with Institute of Information Engineering, Chinese Academy of Sciences, Beijing, China. Y. Liu is with Gaoling School of Artificial Intelligence, Renmin University of China.

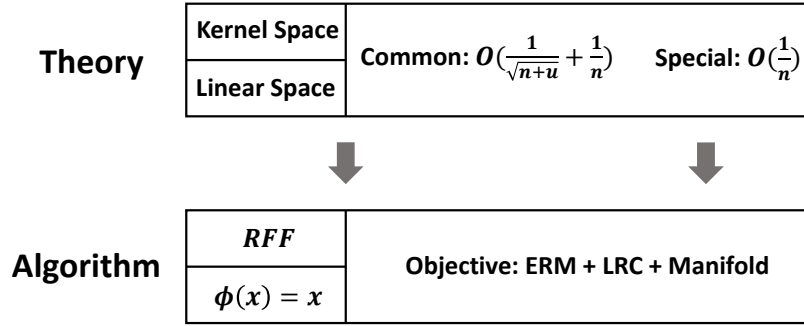


Fig. 1. Main contributions of this paper. We study vector-valued learning from theory to application in both the kernel space and linear space. Here, RFF indicates random Fourier features used to approximate kernel functions. LRC is the tail sum of singular values of the weight matrix. SSL is the Laplacian regularizer.

- Using the contraction inequality (Lemma 4) to directly bound local Rademacher complexity of hypothesis space, we simplify the proof of sharper analysis, while [28] employed a complex derivation from Gaussian complexity to Rademacher complexity.
- A unified framework for learning all kinds of vector-valued functions in the linear space is devised. Specifically, random Fourier features approach [30] is used to approximate kernel functions, avoiding the low efficiency of multiple kernel learning (MKL) [29].
- More experiments are conducted. Beside multi-class classification tasks [28], [29], multi-label learning datasets are also used in this paper. Additionally, we explore the influences of using local Rademacher complexity and unlabeled samples.

## 1.1 Related Work

**Multi-class Classification.** As typical data-independent measures, VC dimension [31] and Natarajan dimension [32] provide conservative multi-class bounds. Data-dependent complexity tools, on the other hand, always yield tighter bounds. As the most common and successful data-dependent measure, Rademacher complexity was first used to analyze the generalizability of multi-class tasks in [33] and then further studied in [2], [34]. The convergence rates of Rademacher complexity based error bounds are usually  $\mathcal{O}(K/\sqrt{n})$ , where  $K$  and  $n$  are the number of classes and the number of labeled samples, respectively. By bridging Gaussian complexity and Rademacher complexity, [24] devised a generalization error bound which exhibits logarithmic dependence on the class size  $\mathcal{O}((\log K)/\sqrt{n})$ . Instead of estimating complexity in the global function space, local Rademacher complexity was proposed to estimate complexity in a more favorable subspace [35], [36] and usually obtains better statistical properties. Under the relatively strict assumption that the derivative of loss function is  $L$ -Lipschitz continuous, our previous work [28] proposed the state-of-the-art error bound for kernel-based multi-class classification using local Rademacher complexity, where the convergence rate is inversely proportional to the number of samples  $n$ . Combining Rademacher complexity with the use of unlabeled data, Maximov et al. proposed a semi-supervised multi-class bound [37], which has a convergence rate of  $\mathcal{O}(\sqrt{K/n} + K\sqrt{K/u})$ , where  $u$  is the number of unlabeled samples. Further, based on local Rademacher complexity, we extended our previous work [28] to a semi-supervised setting in [29] and obtained a tight semi-supervised bound. The convergence rate of this bound is  $\mathcal{O}(K/\sqrt{n+u} + 1/n)$ . Abramovich et al. [38] proved the excess risk bound for multiclass classification with sparse multinomial logistic regression with the rate  $\mathcal{O}(\sqrt{K/n})$ . They further improved it to  $\mathcal{O}(K/n)^{\frac{\alpha+1}{\alpha+2}}$  [38], where  $\alpha \in [0, +\infty)$  is related to the low-noise condition, revealing the probability that most likely class is sufficiently distinguished from others.

**Multi-label Learning.** Data-independent error bounds were developed in [12], [39] using VC-dimension. More recently, the data-dependent complexity Rademacher complexity was introduced into multi-label learning [4], leading to tighter error bounds than the data-independent measures with a convergence rate of  $\mathcal{O}(1/\sqrt{n})$ . Based on theoretical studies, [4] also devised a generic empirical minimization error (ERM) algorithm using the trace norm as a regularizer. Local Rademacher complexity, rather than the global estimate, was used to obtain sharper bounds with a faster convergence rate of  $\mathcal{O}(1/n)$  in [40]. Further, a new algorithm was designed using the tail sum of the predictor’s eigenvalues instead of the trace norm. Both the theoretical analysis and proposed algorithms of [4], [40] are in the linear space, while this paper explores statistical properties and designs a unified algorithm for both the kernel space and linear space.

## 1.2 Contributions

As shown in Figure 1, our main contributions lie in both theory and algorithm. In this paper, we derive novel data-dependent generalization error bounds by making use of local Rademacher complexity and unlabeled data for vector-valued learning. A unified learning framework is further designed and solved by proximal gradient descent on the primal. Extensive experiments verify the effectiveness of the algorithm and support the statistical findings.

**Theoretical Contributions.** We provide theoretical guarantees for learning vector-valued functions in both the kernel space and linear space. Instead of global Rademacher complexity, we exploit *local* Rademacher complexity to improve the convergence rate of excess risk bounds. Unlabeled samples are used to reduce the estimate of local Rademacher complexity. Finally, unified excess risk bounds are established, for which we obtain, for the first time, data-dependent error bounds for semi-supervised vector-valued learning in both the kernel and linear space. To the best of our knowledge, these excess risk bounds are the tightest bounds developed so far for vector-valued learning and can be applied to various vector-valued tasks.

**Algorithmic Contributions.** Motivated by our theoretical analysis, we devise a unified learning framework for vector-valued functions. The framework combines the structural risk minimization (SRM) framework with two additional terms to bound local Rademacher complexity and makes use of unlabeled samples. The tail sum of singular values of the weight matrix in the predictor is used to bound local Rademacher complexity. Under semi-supervised settings, Laplacian regularization is introduced to make use of unlabeled samples, making the algorithm suitable for these settings. Using proximal gradient descent and random features to approximate kernel functions, the algorithm effectively solves the undifferentiable optimization problem on the primal, achieving a good tradeoff between efficiency and accuracy. Experimental results show that our algorithm significantly outperforms compared methods in multi-class classification and multi-label learning tasks.

### 1.3 Outlines

We define vector-valued learning and introduce some preliminaries and notations in Section 2. In Section 3, we derive excess risk bounds for vector-valued learning in both the kernel and linear spaces. We then compare our bounds with existing vector-valued learning generalization error bounds in Section 4. In Section 5, motivated by theoretical analysis, we present a unified learning framework. We empirically validate the theoretical findings and algorithm in Section 6.

## 2 PROBLEM SETTING AND PRELIMINARIES

We define vector-valued problems on input space  $\mathcal{X} = \mathbb{R}^d$  and output space  $\mathcal{Y}$ , which produces vector-valued outputs  $\mathcal{Y} \subseteq \mathbb{R}^K$  (such as multivariate labels). We consider a set of labeled training samples  $\mathcal{D}_l = \{(\mathbf{x}_i, \mathbf{y}_i)\}_{i=1}^n$  i.i.d. drawn from some unknown distribution  $\rho$  over  $\mathcal{X} \times \mathcal{Y}$  and unlabeled samples  $\mathcal{D}_u = \{\mathbf{x}_i\}_{i=n+1}^{n+u}$  i.i.d. sampled according to the marginal distribution  $\rho_{\mathcal{X}}$  of  $\rho$  over  $\mathcal{X}$ . Typically, only a few labeled samples and a large number of unlabeled samples are available, that is,  $n \ll u$ .

### 2.1 The Vector-valued Learning Framework

The goal is to learn a vector-valued estimator  $h : \mathbb{R}^d \rightarrow \mathbb{R}^K$ , which outputs  $K$ -dimensional labels. We define a general hypothesis space for both kernel-based and linear methods

$$\mathcal{H}_p = \left\{ \mathbf{x} \rightarrow h(\mathbf{x}) = \mathbf{W}^T \phi(\mathbf{x}) : \|\mathbf{W}\|_p \leq 1 \right\},$$

where  $\mathbf{W} \in \mathcal{S} \times \mathbb{R}^K$  is the weight matrix,  $\phi(\mathbf{x}) : \mathbb{R}^d \rightarrow \mathcal{S}$  is a feature mapping (linear or non-linear),  $\mathcal{S}$  is the feature space and  $\|\mathbf{W}\|_p$  is a matrix norm to regularize the hypothesis. Specifically, to analyze the generalization performance of vector-valued functions, we use the  $\ell_{2,1}$ -norm  $\|\mathbf{W}\|_{2,1} \leq 1$  in the kernel space and the trace norm  $\|\mathbf{W}\|_* \leq 1$  in the linear space. Then, we present specific estimators for the linear space and kernel space.

We denote the loss function  $\ell : \mathcal{Y} \times \mathcal{Y} \rightarrow \mathbb{R}_+$  to measure the dissimilarity between two elements from vector-valued outputs. Statistical learning is employed to minimize the expected loss

$$\mathcal{E}(h) = \int_{\mathcal{X} \times \mathcal{Y}} \ell(h(\mathbf{x}), \mathbf{y}) d\rho(\mathbf{x}, \mathbf{y}),$$

where  $\ell$  is the loss function and  $h \in \mathcal{H}_p$ . The empirical loss is usually defined as  $\hat{\mathcal{E}}(h) = \frac{1}{n} \sum_{i=1}^n \ell(h(\mathbf{x}_i), \mathbf{y}_i)$ . For the sake of simplicity, we assume that the loss function is bounded  $\ell : \mathcal{Y} \times \mathcal{Y} \rightarrow [0, B]$ , where  $B > 0$  is a constant. This is a common restriction on the loss function, satisfied by the bounded hypothesis. Moreover, we normalize the inner product  $\langle \phi(\mathbf{x}), \phi(\mathbf{x}') \rangle \leq 1$ , so we have  $\sup_{\mathbf{x}, \mathbf{x}' \in \mathcal{X}} \kappa(\mathbf{x}, \mathbf{x}') \leq 1$  for kernel estimators and  $\mathbb{E}[\mathbf{x}^T \mathbf{x}] \leq 1$  for linear estimators.

**Kernel Space.** Let  $\kappa : \mathcal{X} \times \mathcal{X} \rightarrow \mathbb{R}$  be a Mercer kernel with the associated feature map  $\phi$  and reproducing kernel Hilbert space  $H_\kappa$ , where  $\kappa(\mathbf{x}, \mathbf{x}') = \langle \phi(\mathbf{x}), \phi(\mathbf{x}') \rangle$  and  $\phi : \mathbb{R}^d \rightarrow H_\kappa$ , thus  $\mathcal{S} = H_\kappa$ . Unfortunately, kernel methods suffer from high storage and computational burdens, where both time and space complexities are at least quadratic w.r.t the number of training points.

**Approximate Kernel Space.** Random Fourier features (RFF) were proposed in [30] to approximate kernel functions via  $\kappa(\mathbf{x}, \mathbf{x}') \approx \langle \phi(\mathbf{x}), \phi(\mathbf{x}') \rangle$ , where  $\phi(\cdot)$  is an explicit feature mapping  $\phi : \mathbb{R}^d \rightarrow \mathbb{R}^D$ , thus  $\mathcal{S} = \mathbb{R}^D$ . By approximating kernel functions in linear forms, random features obtain excellent statistical properties similar to kernel methods but with a high computational efficiency.

**Linear Space.** The most commonly used linear estimators are directly in the input space, that is  $\mathcal{S} = \mathbb{R}^d$ .

## 2.2 Notations and Assumptions

The space for the loss functions associated with  $\mathcal{H}_p$  is

$$\mathcal{L} = \{\ell(h(\mathbf{x}), \mathbf{y}) \mid h \in \mathcal{H}_p\}. \quad (1)$$

**Definition 1 (Rademacher complexity of the loss space).** Assume  $\mathcal{L}$  is the space for loss functions defined in Equation (1). Then the empirical Rademacher complexity of  $\mathcal{L}$  on  $\mathcal{D}_l$  is:

$$\widehat{\mathcal{R}}(\mathcal{L}) = \frac{1}{n} \mathbb{E}_\epsilon \left[ \sup_{\ell \in \mathcal{L}} \sum_{i=1}^n \epsilon_i \ell(h(\mathbf{x}_i), \mathbf{y}_i) \right], \quad (2)$$

where  $\epsilon_i$ s are random independent Rademacher variables uniformly distributed over  $\{\pm 1\}$ . Its deterministic counterpart is  $\mathcal{R}(\mathcal{L}) = \mathbb{E} \widehat{\mathcal{R}}(\mathcal{L})$ .

**Definition 2 (Local Rademacher complexity of loss space).** For any  $r > 0$ , local Rademacher complexity of  $\mathcal{L}$  is

$$\mathcal{R}(\mathcal{L}_r) = \mathcal{R}(\{\ell_h \mid \ell_h \in \mathcal{L}, \mathbb{E}(\ell_h - \ell_{h^*})^2 \leq r\}), \quad (3)$$

where  $\ell_{h^*}$  represents the minimal expected loss.

From (2) to (3), a smaller class  $\mathcal{L}_r \subseteq \mathcal{L}$  is selected by a ball around the minimal expected loss  $\ell_{h^*}$  with a fixed radius  $r$ . The corresponding localized hypothesis space is

$$\mathcal{H}_r = \{h \mid h \in \mathcal{H}_p, \mathbb{E}(\ell_h - \ell_{h^*})^2 \leq r\}. \quad (4)$$

Definitions 1 and 2 demonstrate that Rademacher complexity of the loss space is output-dependent, such that the empirical counterparts can be estimated only on the labeled samples  $\mathcal{D}_l$ . In the following definition, we introduce the notion of Rademacher complexity of the hypothesis space, which is output-independent and can be estimated on both the labeled samples  $\mathcal{D}_l$  and unlabeled samples  $\mathcal{D}_u$ .

**Definition 3 (Local Rademacher complexity of hypothesis space).** Assume that the localized hypothesis space  $\mathcal{H}_r$  is defined as in (4). The empirical local Rademacher complexity of  $\mathcal{H}_r$  on both labeled and unlabeled samples  $\mathcal{D}_l \cup \mathcal{D}_u$  is defined as:

$$\widehat{\mathcal{R}}(\mathcal{H}_r) = \frac{1}{n+u} \mathbb{E}_\epsilon \left[ \sup_{h \in \mathcal{H}_r} \sum_{i=1}^{n+u} \sum_{j=1}^K \epsilon_{ik} h_j(\mathbf{x}_i) \right],$$

where  $h_j(\mathbf{x}_i)$  is the  $j$ -th value in the vector-valued function  $h(\mathbf{x}_i)$  with  $K$  outputs and  $\epsilon_{iks}$  are  $(n+u) \times K$  Rademacher variables. The deterministic counterpart is  $\mathcal{R}(\mathcal{H}_r) = \mathbb{E} \widehat{\mathcal{R}}(\mathcal{H}_r)$ .

Consider the loss function  $\ell$  is bounded  $\ell \in [0, B]$  and satisfies the following condition.

**Assumption 1.** We assume that the loss function  $\ell : \mathcal{Y} \times \mathcal{Y} \rightarrow \mathbb{R}_+$  is  $L$ -Lipschitz continuous for  $\mathbb{R}^K$  equipped with the  $\ell_2$ -norm. There holds

$$|\ell(h(\mathbf{x}), \mathbf{y}) - \ell(h'(\mathbf{x}'), \mathbf{y})| \leq L \|h(\mathbf{x}) - h'(\mathbf{x}')\|_2,$$

where  $(\mathbf{x}, \mathbf{y}) \in \mathcal{X} \times \mathcal{Y}$ ,  $\forall \mathbf{x}' \in \mathcal{X}$  and  $h, h' : \mathcal{X} \rightarrow \mathcal{Y}$ .

This assumption is standard in vector-valued learning and can be extended to structured prediction [25]. Using the Lipschitz condition and contraction lemma for Rademacher complexity of vector-valued learning proven in [25], [26], we further establish the connection between local Rademacher complexity of the loss space and hypothesis space.

## 3 THEORETICAL ANALYSIS

In this section, we study the generalization ability of vector-valued learning. Firstly, a general excess risk bound is derived using local Rademacher complexity and unlabeled samples. Then, for the kernel hypotheses, an estimate of local Rademacher complexity is explored based on eigenvalues decomposition of the normalized kernel matrix. Thus, an explicit excess risk bound is derived. Meanwhile, for the linear hypotheses, we bound local Rademacher complexity based on singular values decomposition of the weight matrix  $\mathbf{W}$  and then provide an explicit excess risk bound. Our analysis is general and applicable to a broad family of vector-valued functions, as long as the loss function is Lipschitz continuous and bounded.

### 3.1 General Bound for Local Rademacher Complexity

*Lemma 4 (Lemma 5 of [25]).* Under Assumption 1, the following contraction inequality exists

$$\mathcal{R}(\mathcal{L}_r) \leq \sqrt{2}L\mathcal{R}(\mathcal{H}_r).$$

The contraction lemma above has been proven based on Khintchine inequalities in Lemma 5 of [25] and Theorem 3 of [26]. The contraction inequality in Lemma 4 is the key tool for analyzing vector-valued output functions, bridging the gap between Rademacher complexity of the loss space and hypothesis space. We can then make use of unlabeled data because the richness measure of the hypothesis space is output-independent, always leading to tighter error bounds.

*Theorem 5 (Excess risk bound of vector-valued learning).* Assume the loss function satisfies Assumption 1. Let  $\psi(r)$  be a sub-root function and  $r^*$  be the fixed point of  $\psi$ . Fix  $\delta \in (0, 1)$  and assume that, for any  $r \geq r^*$ ,

$$\psi(r) \geq \sqrt{2}BL\mathcal{R}(\mathcal{H}_r). \quad (5)$$

Then, with a probability of at least  $1 - \delta$ ,

$$\mathcal{E}(\hat{h}) - \mathcal{E}(h^*) \leq \frac{705}{B}r^* + \frac{49B \log(1/\delta)}{n}, \quad (6)$$

where  $\hat{h}, h^*$  are the estimators with the minimal empirical loss and the minimal expected loss, respectively.

Above theorem provides a general excess risk bound for semi-supervised vector-valued functions based on local Rademacher complexity. The classic local Rademacher complexity based bounds [35] estimate the complexity on the loss space  $\mathcal{R}(\mathcal{L}_r)$ . Note that  $\mathcal{R}(\mathcal{L}_r)$  is label-dependent so can only be estimated on labeled samples  $\mathcal{D}_l$ , whose convergence rate is  $\mathcal{O}(1/\sqrt{n})$ . In contrast, we estimate Rademacher complexity of the hypothesis space  $\mathcal{R}(\mathcal{H}_r)$ , which is label-independent and so it can be estimated on both labeled samples  $\mathcal{D}_l$  and unlabeled samples  $\mathcal{D}_u$ , where the convergence rate is  $\mathcal{O}(1/\sqrt{n+u})$ . Therefore, using the contraction inequality in Lemma 4, we introduce  $\mathcal{R}(\mathcal{H}_r)$  instead of  $\mathcal{R}(\mathcal{L}_r)$  to derive tighter error bounds.

*Remark 6.* When there is no labeled data, setting  $u = 0$  coincides with local Rademacher complexity bounds in supervised settings [28]. The convergence rate of these bounds depends on the  $\mathcal{R}(\mathcal{H}_r)$  and  $\mathcal{O}(1/n)$  terms, so it cannot be faster than  $\mathcal{O}(1/n)$ . The number of unlabeled instances plays a key role in making the error bounds close to  $\mathcal{O}(1/n)$  during the generalization analysis.

### 3.2 Excess Risk Bound for Kernel Hypotheses

In this section, we study the generalization performance of vector-valued functions with kernel hypotheses. We first present an estimate of local Rademacher complexity on all data in Theorem 7, which depends primarily on the tail sum of the eigenvalues of the normalized kernel matrix. Then, we derive an explicit excess risk bound based on local Rademacher complexity (Corollary 9) for vector-valued functions with a faster convergence rate, by applying Theorem 7 to Theorem 5. For kernel estimators, we consider  $\ell_{2,1}$ -norm to regularize  $\mathbf{W}$ , where  $\|\mathbf{W}\|_{2,1} = \sum_{k=1}^K \|\mathbf{W}_{\cdot k}\|_2$  and  $\mathbf{W}_{\cdot k}$  represents the  $k$ -th column of  $\mathbf{W}$ .

*Theorem 7 (Local Rademacher complexity for kernel estimators).* Consider  $\|\mathbf{W}\|_{2,1} \leq 1$  as the normalization. Let eigenvalue decomposition be  $\kappa(\mathbf{x}, \mathbf{x}') = \sum_{j=1}^{\infty} \lambda_j \psi_j(\mathbf{x})^T \psi_j(\mathbf{x}')$ , where its eigenvalues be  $(\lambda_j)_{j=1}^{\infty}$  in a nonincreasing order. For any  $r > 0$ , there holds

$$\mathcal{R}(\mathcal{H}_r) \leq 2 \sqrt{\frac{1}{n+u} \min_{\theta \geq 0} \left( \frac{\theta r}{4L^2} + \sum_{j>\theta} \lambda_j \right)}.$$

Theorem 7 demonstrates that local Rademacher complexity is determined by the tail sum of eigenvalues, where the eigenvalues are truncated at the "cut-off point"  $\theta$ .

*Remark 8.* Notably, local Rademacher complexity is independent from the number of classes  $K$ , because the constraints on  $\mathbf{W} \in \mathcal{S} \times \mathbb{R}^K$  (e.g.  $\|\mathbf{W}\|_{2,1} \leq 1$ ) are actually related to the dimensionality of the output space  $K$ . When  $K$  is bigger, the constraints are relatively stricter.

*Corollary 9 (Excess risk bound for kernel estimators).* Assume the loss function satisfies Assumption 1 and kernel estimators satisfy  $\sup_{\mathbf{x} \in \mathcal{X}} \kappa(\mathbf{x}, \mathbf{x}) \leq 1$  and  $\|\mathbf{W}\|_{2,1} \leq 1$ . With a probability of at least  $1 - \delta$ , it holds that

$$\mathcal{E}(\hat{h}) - \mathcal{E}(h^*) \leq c_{L,B} \left( r^* + \frac{\log(1/\delta)}{n} \right), \quad (7)$$

where, for the fixed point, it holds that

$$r^* \leq \min_{\theta \geq 0} \left( \frac{\theta}{n+u} + \sqrt{\frac{1}{n+u} \sum_{j>\theta} \lambda_j} \right),$$

where  $c_{L,B}$  a constant only depending on  $L$  and  $B$ .

The convergence rate of the above bound depends on the quantity  $\sqrt{\frac{1}{n+u} \sum_{j>\theta} \lambda_j}$ , which can be estimated as follows:

**1) The worst case (when  $\theta = 0$ ).** The complexity degrades into the *global* Rademacher complexity, depending on the trace of the kernel  $\kappa$ . Then, the convergence rate of excess risk bound is  $\mathcal{E}(\hat{h}) - \mathcal{E}(h^*) = \mathcal{O}\left(\sqrt{\frac{1}{n+u} + \frac{1}{n}}\right)$ .

**2) Finite-rank kernel.** When the kernel  $\kappa$  has a finite rank  $\theta$  such that its eigenvalues satisfy  $\lambda_j = 0$  for all  $j > \theta$ , the tail sum of eigenvalues is zero. Indeed, a lot of common kernels are finite-rank kernels, e.g. the linear kernel and polynomial kernel. The linear kernel  $\kappa(\mathbf{x}, \mathbf{x}') = \langle \mathbf{x}, \mathbf{x}' \rangle$  has a rank of at most  $\theta = d$ . For a polynomial kernel  $\kappa(\mathbf{x}, \mathbf{x}') = (\langle \mathbf{x}, \mathbf{x}' \rangle + 1)^p$  with degree  $p$ , its rank is at most  $\theta = p + 1$ . Thus, the rate of the fixed point is inversely proportional to the number of samples, that is  $r^* = \mathcal{O}\left(\frac{\theta}{n+u}\right)$ .

**3) Exponentially decaying eigenvalues.** When the eigenvalues of the normalized kernel matrix  $\mathbf{K}$  decay exponentially  $\sum_{j>\theta} \lambda_j = \mathcal{O}(\exp(-\theta))$ , such as for Gaussian kernels [35], [41], then by truncating a thresholding with  $\theta = \log(n+u)$  it holds that  $r^* = \mathcal{O}\left(\frac{\log(n+u)}{n+u}\right)$ .

Both finite-rank kernels and kernels with exponentially decaying eigenvalues have an  $r^*$  that mainly depends on  $\mathcal{O}(1/(n+u))$ , which is much smaller than  $\mathcal{O}(1/n)$ . In these cases, the excess risk bound (7) provides a linear dependence on the labeled sample size  $\mathcal{E}(\hat{h}) - \mathcal{E}(h^*) = \mathcal{O}\left(\frac{1}{n}\right)$ , yielding much stronger generalization bounds. A similar analytical procedure is also used in classic local Rademacher complexity literature [35], [40], [42].

### 3.3 Excess Risk Bound for Linear Hypotheses

In this section, we study the local Rademacher complexity bound for linear hypotheses  $h(\mathbf{x}) = \mathbf{W}^T \mathbf{x}$ , using the singular values decomposition (SVD) of the weight matrix  $\mathbf{W}$ . The result (Theorem 10) shows that local Rademacher complexity can be bounded by the tail sum of the singular values of  $\mathbf{W}$ . Combining Theorem 5 and Theorem 10, we obtain a tighter generalization error bound (Corollary 12).

**Theorem 10 (Local Rademacher complexity for linear estimators).** Let the SVD decomposition be  $\mathbf{W} = \mathbf{U}\mathbf{\Sigma}\mathbf{V}^T$ .  $\mathbf{U}$  and  $\mathbf{V}$  are unitary matrices, and  $\mathbf{\Sigma}$  is diagonal with singular values  $\{\tilde{\lambda}_j\}$  in descending order. Under Assumption 1, assuming  $\mathbb{E}[\mathbf{x}^T \mathbf{x}] \leq 1$  and  $\|\mathbf{W}\|_* \leq 1$ , the local Rademacher complexity  $\mathcal{R}(\mathcal{H}_r)$  for linear hypotheses is upper bounded by

$$\mathcal{R}(\mathcal{H}_r) \leq 2 \sqrt{\frac{1}{n+u} \min_{\theta \geq 0} \left( \frac{\theta r}{4L^2} + \sum_{j>\theta} \tilde{\lambda}_j^2 \right)}.$$

The above theorem estimates local Rademacher complexity for linear estimators. We find that the first term of the right side of the inequality  $\theta r/(4L^2)$  is a constant, such that local Rademacher complexity is determined by the tail sum of squared singular values of the weight matrix  $\mathbf{W}$ .

**Remark 11.** For the kernel hypotheses, local Rademacher complexity can be bounded by the tail sum of the eigenvalues of the normalized kernel matrix  $\mathbf{K}$  [28], [35], [42]. Similarly, for the linear hypotheses, Theorem 10 shows that local Rademacher complexity can be bounded by the singular values of the weight matrix  $\mathbf{W}$ .

**Corollary 12 (Excess risk bound for linear estimators).** Assume that the loss function satisfies Assumption 1. Let  $\mathbb{E}[\mathbf{x}^T \mathbf{x}] \leq 1$  and the trace norm  $\|\mathbf{W}\|_* \leq 1$ . With a probability of at least  $1 - \delta$ , it holds that

$$\mathcal{E}(\hat{h}) - \mathcal{E}(h^*) \leq \tilde{c}_{L,B} \left( \tilde{r}^* + \frac{\log(1/\delta)}{n} \right), \quad (8)$$

where, for the fixed point, it holds that

$$\tilde{r}^* \leq \min_{\theta \geq 0} \left( \frac{\theta}{n+u} + \sqrt{\frac{1}{n+u} \sum_{j>\theta} \tilde{\lambda}_j^2} \right),$$

where  $(\tilde{\lambda}_j)_{j=1}^\infty$  are the singular values of  $\mathbf{W}$  and  $\tilde{c}_{L,B}$  is a constant only depending on  $L$  and  $B$ .

The convergence rate of Corollary 12 depends on the quantity  $\sqrt{\frac{1}{n+u} \sum_{j>\theta} \tilde{\lambda}_j^2}$  and we estimate it as follows:

**1) The worst case ( $\theta = 0$ ).** The fixed point  $\tilde{r}^*$  becomes relevant to *global* Rademacher complexity, at  $\mathcal{O}(1/\sqrt{n+u})$ . Thus, the convergence rate is  $\mathcal{E}(\hat{h}) - \mathcal{E}(h^*) = \mathcal{O}\left(\frac{1}{\sqrt{n+u}} + \frac{1}{n}\right)$ .

**2) Faster convergence.** Similar to the analysis in Subsection 3.2, when  $\mathbf{W}$  has a finite rank or its eigenvalues decay exponentially, the fixed point  $\tilde{r}^*$  mainly depends on  $\tilde{r}^* \leq \theta/(n+u)$  in (8). We obtain better results with a fast convergence rate  $\mathcal{E}(\hat{h}) - \mathcal{E}(h^*) = \mathcal{O}\left(\frac{1}{n}\right)$ . Similar theoretical results for *linear* estimators were presented for multi-label [40] and multi-class in our previous work [29].

Bounds	Worst Case	Special Case
GRC for VV [25]	Kernel: $\mathcal{O}(\sqrt{\frac{\log K}{n}})$	Linear: $\mathcal{O}(\sqrt{\frac{K}{n}})$
GRC for VV [26]	Kernel: $\mathcal{O}(\frac{1}{\sqrt{n}})$	Linear: $\mathcal{O}(\sqrt{\frac{K}{n}})$
LRC for Kernel VV (Corollary 9) †‡	$\mathcal{O}(\frac{1}{\sqrt{n+u}} + \frac{1}{n})$	$\mathcal{O}(\frac{1}{n})$
LRC for Linear VV (Corollary 12) †‡	$\mathcal{O}(\frac{1}{\sqrt{n+u}} + \frac{1}{n})$	$\mathcal{O}(\frac{1}{n})$

TABLE 1

Data-dependent error bounds for vector-valued functions (VV). † indicates with unlabeled data and ‡ represents excess risk bounds.

Bounds	Worst Case	Special Case
GRC for Kernel MC [2]	$\mathcal{O}(\frac{K}{\sqrt{n}})$	
GRC for Kernel MC [24], [43]	$\mathcal{O}(\frac{\log K}{\sqrt{n}})$	
GRC for Kernel MC [37] †	$\mathcal{O}(\sqrt{\frac{K}{n}} + K\sqrt{\frac{K}{u}})$	
GRC for Linear MC [38] ‡	$\mathcal{O}(\frac{K}{n})^{\alpha+1/\alpha+2}$	
LRC for Kernel MC [28]	$\mathcal{O}(\frac{\log^2 K}{n})$	
LRC for Linear MC [29] †	$\mathcal{O}(\frac{K}{\sqrt{n+u}} + \frac{1}{n})$	$\mathcal{O}(\frac{1}{n})$
LRC for Kernel VV (Corollary 9) †‡	$\mathcal{O}(\frac{1}{\sqrt{n+u}} + \frac{1}{n})$	$\mathcal{O}(\frac{1}{n})$
LRC for Linear VV (Corollary 12) †‡	$\mathcal{O}(\frac{1}{\sqrt{n+u}} + \frac{1}{n})$	$\mathcal{O}(\frac{1}{n})$

TABLE 2

Data-dependent error bounds for multi-class classification (MC). † indicates with unlabeled data and ‡ represents excess risk bounds. The value  $\alpha \in [0, +\infty)$  is related to the low-noise condition [38].

**Remark 13.** The tail sum of eigenvalues or singular values are often used to bound local Rademacher complexity [35], [40], [42]. As discussed in [42], the choice of threshold  $\theta$  is very important. If  $\theta$  is too small, the *local* Rademacher complexity will be close to the *global* Rademacher complexity. If  $\theta$  is too big, the *local* Rademacher complexity will be nearly constant. For the finite-rank matrix, we simply set  $\theta$  equal to rank, so the tail sum is zero. For other cases, the optimal  $\theta$  is obtained by making two terms in Theorem 7 and Theorem 10 equal, typically  $\frac{\theta r}{4L^2} = \sum_{j>\theta} \lambda_j$  for the kernel hypotheses and  $\frac{\theta r}{4L^2} = \sum_{j>\theta} \tilde{\lambda}_j^2$  for the linear hypotheses.

## 4 SPECIAL CASES AND COMPARISONS

In this section, we first introduce the typical data-dependent error bounds of general vector-valued functions and compare them with our bounds. Then, we present traditional works for two special cases, multi-class classification and multi-label learning, and then compare their statistical properties with ours. Specifically, from the following comparisons, our error bounds are *excess risk bounds* while others are *generalization error bounds*. The *excess risk bound* is defined as  $\mathcal{E}(\hat{h}) - \mathcal{E}(h^*)$ , while the *generalization error bound* measures the difference between the expected loss and the empirical loss for any hypotheses  $\mathcal{E}(h) - \hat{\mathcal{E}}(h)$ . It is more difficult to obtain *excess risk bounds*.

### 4.1 General Vector-valued Functions

In this paper, the contraction inequality in Lemma 4 is a key step in our analysis to connect Rademacher complexity of loss function classes and Rademacher complexity of the hypothesis space. Table 1 shows comparisons of data-dependent error bounds. For kernelized vector-valued functions, the convergence rate of error bounds in [25] and [26] are  $\mathcal{O}(\sqrt{\log K/n})$  and  $\mathcal{O}(\sqrt{1/n})$  respectively, while we improve the kernel bounds to  $\mathcal{O}(1/\sqrt{n+u} + 1/n)$ . For linear vector-valued functions, the learning error rates of [25] and [26] are both  $\mathcal{O}(\sqrt{K/n})$ , while the theoretical analysis in Corollary 12 provides a much sharper learning rate, even in the worst case, of  $\mathcal{O}(1/\sqrt{n+u} + 1/n)$ . What's more, in the benign cases, the convergence rates of vector-valued learning in both the kernel space and linear space are  $\mathcal{O}(1/n)$ , which is much faster than the rate of error bounds in [25], [26]. Meanwhile, our bounds are independent from the vector size  $K$ , thus they are more suitable when  $K$  is large. To make the hypothesis space smaller, we explore the *local* Rademacher complexity instead of the *global* one. Meanwhile, to reduce the output-independent complexity  $\mathcal{R}(\mathcal{H}_r)$ , we make use of unlabeled samples. Based on these two aspects, we obtain significant statistical gains.

### 4.2 Special Case: Multi-class Classification

Based on data-dependent richness measures, the generalization ability of multi-class classification has been well-studied [24], [37], [44]. As illustrated in Table 2, our excess bounds are among the sharpest results both in the kernel space and

Bounds	Worst Case	Special Case
GRC for Linear ML [4]	$\mathcal{O}(\frac{1}{\sqrt{n}})$	
LRC for Linear ML [40]	$\mathcal{O}(\frac{1}{\sqrt{n}})$	$\mathcal{O}(\frac{1}{n})$
LRC for Kernel VV (Corollary 9) † ‡	$\mathcal{O}(\frac{1}{\sqrt{n+u}} + \frac{1}{n})$	$\mathcal{O}(\frac{1}{n})$
LRC for Linear VV (Corollary 12) † ‡	$\mathcal{O}(\frac{1}{\sqrt{n+u}} + \frac{1}{n})$	$\mathcal{O}(\frac{1}{n})$

TABLE 3

Data-dependent error bounds for multi-label learning (ML). † indicates with unlabeled data and ‡ represents excess risk bounds.

linear space. Generalization error bounds using Rademacher complexity for multi-class classification were explored in [2], [33], [44] and the convergence rate of these error bounds is  $\mathcal{O}(K/\sqrt{n})$ . Using Gaussian complexity (GC) and Slepian’s Lemma, a generalization error bound with logarithmic dependence on  $K$  was derived in [24], [43], whose convergence rate is  $\mathcal{O}(\log K/\sqrt{n})$ . Making use of unlabeled instances, Maximov et al. presented a data-dependent error bound for semi-supervised multi-class classification with the rate  $\mathcal{O}(\sqrt{K/n} + K\sqrt{K/u})$  [37]. With low-noise condition, [38] provide the generalization error bound for multiclass logistic regression with the rate  $\mathcal{O}(K/n)^{\alpha+1/\alpha+2}$ , where  $\alpha$  reflects the probability that the most likely class is sufficiently distinguished from others. Only when  $\alpha = \infty$  that the most likely class is naturally distinguished from others, the convergence rate can achieve  $\mathcal{O}(K/n)$ , while our error bounds can achieve the convergence rates  $\mathcal{O}(1/n)$  without the low-noise condition.

Although *global* Rademacher complexity is widely used in generalization analysis, it does not take into consideration the fact that the hypothesis selected by a learning algorithm typically belongs to a small favorable subset of all hypotheses [35], [42]. In contrast, local Rademacher complexity evaluates richness on a small subset of the hypothesis space, which is often used to obtain better error bounds for binary classification and regression. Our previous work [28] introduced local Rademacher complexity into multi-class classification and obtained a reciprocal dependence on the number of labeled samples  $n$  for the first time. However, this paper is quite different from our previous work [28] in both its conditions and technical details:

**1) Milder condition.** The previous work used a more strict condition requiring that the loss function be  $L$ -smooth ( $L$ -Lipschitz continuous on the first-order derivative). In contrast, as demonstrated in Assumption 1, this paper just assumes the loss function itself is bounded and continuous.

**2) Concise proof details.** The previous work reached local Rademacher complexity in steps:  $\text{GC} \Rightarrow \text{GRC} \Rightarrow \text{LRC}$ , based on key tools including Slepian’s Lemma, the connection lemma (Lemma 2.2 of [45]) and an  $L$ -smooth assumption. Here, GC represents Gaussian complexity, while GRC and LRC are global and local Rademacher complexity. In contrast, this paper estimates LRC directly via Lemma 4.

**3) Implicitly dependent on the number of classes  $K$ .** Traditional Rademacher complexity bounds of multi-class classification are directly dependent on  $K$  when they estimate  $\mathcal{R}(\mathcal{H})$ , while this paper proves that  $\mathcal{R}(\mathcal{H}_r)$  is implicitly dependent on  $K$  due to local Rademacher complexity and the regularization  $\|\mathbf{W}\|_p \leq 1$ .

### 4.3 Special Case: Multi-Label Learning

The *global* Rademacher complexity was introduced to the generalization analysis of multi-label learning in [4], obtaining generalization error bounds of  $\mathcal{O}(1/\sqrt{n})$ . Generally, the *global* Rademacher complexity is bounded by the trace norm of  $\mathbf{W}$ . Further, using the *local* Rademacher complexity, [40] improved the error bounds. Local Rademacher complexity of multi-label learning can be determined by the tail sum of singular values of  $\mathbf{W}$ , where a fast convergence rate  $\mathcal{O}(1/n)$  is obtained when the rank of  $\mathbf{W}$  is finite or its singular values decay exponentially. Both [4] and [40] explored the generalization ability of multi-label learning in the linear space, while our theoretical results include both the linear and nonlinear estimators.

Table 3 compares data-dependent generalization bounds for multi-label learning, showing that our results are much better than former works due to the use of local Rademacher complexity and unlabeled data.

## 5 ALGORITHM

Based on our theoretical analysis, we present a unified learning framework to minimize the empirical loss, local Rademacher complexity and manifold regularization at the same time. Local Rademacher complexity is bounded by the tail sum of eigenvalues for kernel methods and singular values for linear models. Manifold regularization is employed to make use of unlabeled instances. Then, to solve the minimization objective, with adaptive learning rates, we use proximal gradient descent optimization methods and update partial singular values according to thresholding.

### 5.1 Learning Framework

We modify the structural risk minimization (SRM) learning framework with two additional terms: a manifold regularizer to make use of unlabeled samples and a regularizer term to bound local Rademacher complexity.



### 5.1.1 Manifold Regularization

Consider a similarity matrix  $\mathbf{S}$  on all  $n + u$  samples, where  $\mathbf{S}_{ij}$  represents the similarity between  $\mathbf{x}_i$  and  $\mathbf{x}_j$ , defined by the binary weights for k-nearest neighbors or the heat kernel  $\mathbf{S}_{ij} = \exp(-\|\mathbf{x}_i - \mathbf{x}_j\|^2/\sigma^2)$ . To make use of unlabeled data, we define the cost function (manifold regularization) as

$$E(h) = \sum_{i,j=1}^{n+u} \mathbf{S}_{ij} \|h(\mathbf{x}_i) - h(\mathbf{x}_j)\|_2^2 = \text{trace}(\mathbf{W}^T \tilde{\mathbf{X}} \mathbf{L} \tilde{\mathbf{X}}^T \mathbf{W}), \quad (9)$$

where  $\tilde{\mathbf{X}} \in \mathbb{R}^{D \times (n+u)}$  corresponds to a feature mapping  $\phi$  on all samples, graph Laplacian  $\mathbf{L} = \mathbf{D} - \mathbf{S}$  and  $\mathbf{D}$  is a diagonal matrix with  $\mathbf{D}_{ii} = \sum_{j=1}^{n+u} \mathbf{S}_{ij}$ . The cost function (9) is used as a regularizer for multi-class classification [46], [47] and multi-label learning [48]. Anis et al. provided a sampling theory for graph-based semi-supervised learning [49].

### 5.1.2 Local Rademacher Complexity Term

Motivated by theoretical results (Corollary 9 and Corollary 12), we use the tail sum of the eigenvalues of the normalized kernel matrix  $\mathbf{K}$  or the tail sum of the squared singular values of weight matrix  $\mathbf{W}$  to bound local Rademacher complexity. Note that the minimization of the tail sum of singular values  $\sum_{j>\theta} \tilde{\lambda}_j(\mathbf{W})$  is equivalent to the tail sum of squared singular values  $\sum_{j>\theta} \tilde{\lambda}_j^2(\mathbf{W})$ . For the sake of simplicity, we use singular values form. The regularizer used to minimize local Rademacher complexity is

$$T(h) = \begin{cases} \sum_{j>\theta} \lambda_j(\mathbf{K}), & \text{for kernel hypotheses,} \\ \sum_{j>\theta} \tilde{\lambda}_j(\mathbf{W}), & \text{for linear hypotheses,} \end{cases} \quad (10)$$

where  $\lambda_j(\mathbf{K})$  represents the  $j$ -th largest eigenvalue of the kernel matrix  $\mathbf{K}$  and  $\tilde{\lambda}_j(\mathbf{W})$  represents the  $j$ -th largest singular value of  $\mathbf{W}$ .

### 5.1.3 Minimization Objective

Then, combining the ERM learning framework with the Laplacian regularization (9) and local Rademacher complexity term (10), we define the minimization objective as

$$\arg \min_{h \in \mathcal{H}_r} \underbrace{\frac{1}{n} \sum_{i=1}^n \ell(h(\mathbf{x}_i), \mathbf{y}_i) + \tau_A \|\mathbf{W}\|_F^2 + \tau_I E(h) + \tau_S T(h)}_{g(\mathbf{W})}, \quad (11)$$

where  $\tau_A$ ,  $\tau_I$  and  $\tau_S$  are regularization parameters,  $E(h)$  is the Laplacian regularization and  $T(h)$  is the regularizer on local Rademacher complexity.

For kernel hypotheses, the tail sum of the eigenvalues of the kernel is commonly used to estimate local Rademacher complexity. However, the tail sum of eigenvalues for one single kernel is a constant, so it has no influence on the learning model if we add this term to the objective. However, local Rademacher complexity of multiple kernel learning (MKL) is undetermined, and thus our previous work [28] introduced local Rademacher complexity to improve the performance of multi-class MKL. Yet, the optimization of multi-class MKL was overly complicated and inefficient.

In this paper we adopt efficient random Fourier features to approximate single kernel methods [30] rather than using ineffective MKL. We then define local Rademacher complexity term in a general form in (10),  $T(h) = \sum_{j>\theta} \tilde{\lambda}_j(\mathbf{W})$ , for both linear estimators and approximate kernel estimators.

## 5.2 Optimization

Inspired by generalized SVT methods, our previous work [29] proposed a partly singular values thresholding learning framework based on the proximal gradient for the linear hypotheses. To solve the minimization (11) in both the linear hypothesis space and approximate kernel hypothesis space, in this paper, we extend the previous algorithm with feature mappings and adaptive learning rates. As illustrated in Algorithm 1, updating  $\mathbf{W}$  requires two steps: (1) updating  $\mathbf{W}$  using mini-batch gradient descent on  $g(\mathbf{W})$ ; (2) updating partial singular values to minimize  $\sum_{j>\theta} \tilde{\lambda}_j(\mathbf{W})$ .

### 5.2.1 Updating $\mathbf{W}$ with Proximal Gradient Descent

Consider the mini-batch gradient descent with  $m$  samples,

$$\mathbf{Q}_t = \mathbf{W}_t - \eta_t \nabla g(\mathbf{W}_t), \quad (14)$$

where  $\nabla g(\mathbf{W}_t)$  is the derivative of differentiable terms

$$\nabla g(\mathbf{W}_t) = \frac{1}{m} \sum_{i=1}^m \frac{\partial \ell(h(\mathbf{x}_i), \mathbf{y}_i)}{\partial \mathbf{W}_t} + 2\tau_A \mathbf{W}_t + 2\tau_I \tilde{\mathbf{X}} \mathbf{L} \tilde{\mathbf{X}}^T \mathbf{W}_t. \quad (15)$$

Here,  $\eta_t$  is the learning rate for the  $t$ -iteration. For each iteration, we first update the gradients on  $m$  randomly sampled examples.

**Algorithm 1** Semi-supervised vector-valued learning (LSVV)

**Input:** Normalized datasets  $\mathcal{D}_l$  and  $\mathcal{D}_u$ . Initialized matrix  $\mathbf{W}_1 = \mathbf{0}$  and variables  $G_1 = M_1 = 0$ . Stop iteration number  $T$ .  
 Feature mapping  $\phi$ . Parameters:  $\theta, \tau_A, \tau_I, \tau_S, \eta_t$ .

**Output:**  $\mathbf{W}_{T+1}$

Compute Laplacian matrix  $\mathbf{L}$  on both  $\mathcal{D}_l$  and  $\mathcal{D}_u$ .

Feature mapping on all samples:  $\tilde{\mathbf{X}} = \phi(\mathbf{X})$ .

**for**  $t = 1, 2, \dots, T$  **do**

Select a batch of pairs uniformly  $(\mathbf{x}_i, \mathbf{y}_i)_{i=1}^m \in \mathcal{D}_l$ .

Compute the gradient  $\nabla g(\mathbf{W}_t)$  on sample  $\mathbf{x}_i$ ,

$$\nabla g(\mathbf{W}_t) = \frac{1}{m} \sum_{i=1}^m \frac{\partial \ell(h(\mathbf{x}_i), \mathbf{y}_i)}{\partial \mathbf{W}_t} + 2\tau_A \mathbf{W}_t + 2\tau_I \tilde{\mathbf{X}} \mathbf{L} \tilde{\mathbf{X}}^T \mathbf{W}_t.$$

Update the gradient only use  $g(\mathbf{W})$

$$\mathbf{Q}_t = \mathbf{W}_t - \eta_t \nabla g(\mathbf{W}_t). \quad (12)$$

Compute the SVD decomposition  $\mathbf{U} \mathbf{\Sigma} \mathbf{V}^T = \mathbf{Q}_t$ .

Update  $\mathbf{W}_{t+1}$  by reducing first  $\theta$  singular values

$$\mathbf{W}_{t+1} = \mathbf{U} \mathbf{\Sigma}_\tau^\theta \mathbf{V}^T \quad \text{where } \tau = \eta_t \tau_S \quad (13)$$

**end for**

### 5.2.2 Updating $\mathbf{W}$ with Singular Values Thresholding

Consider singular value decomposition  $\mathbf{U} \mathbf{\Sigma} \mathbf{V}^T = \mathbf{Q}_t$ , where  $\mathbf{U} \in \mathbb{R}^{d \times d}$  and  $\mathbf{V} \in \mathbb{R}^{K \times K}$  are orthogonal matrices, and  $\mathbf{\Sigma}$  is diagonal with nonincreasing singular values

$$\mathbf{W}_{t+1} = \mathbf{U} \mathbf{\Sigma}_\tau^\theta \mathbf{V}^T. \quad (16)$$

Here, with  $\tau = \eta_t \tau_S$ , only first  $\theta$  singular values are updated

$$(\mathbf{\Sigma}_\tau^\theta)_{jj} = \begin{cases} |\Sigma_{jj} - \tau|_+ & j \leq \theta, \\ \Sigma_{jj}, & j > \theta. \end{cases}$$

### 5.3 Approximate Kernels with Random Features

To obtain better performance, we use random Fourier features to approximate a shift-invariant kernel

$$\kappa(\mathbf{x}, \mathbf{x}') = \int_{\mathbb{R}^d} e^{i\boldsymbol{\omega}^T(\mathbf{x} - \mathbf{x}')} s(\boldsymbol{\omega}) d\boldsymbol{\omega}. \quad (17)$$

We then define an explicit feature mapping  $\phi : \mathbb{R}^d \rightarrow \mathbb{R}^D$  as

$$\phi(\mathbf{x}) = \sqrt{\frac{2}{D}} \cos(\boldsymbol{\Omega}^T \mathbf{x} + \mathbf{b}), \quad (18)$$

where  $\boldsymbol{\Omega} = [\boldsymbol{\omega}_1, \dots, \boldsymbol{\omega}_D] \in \mathbb{R}^{d \times D}$  is a frequency matrix whose columns are drawn i.i.d. from the density measure  $(\boldsymbol{\omega}_i)_{i=1}^D \stackrel{\text{i.i.d.}}{\sim} s(\boldsymbol{\omega})$  and  $\mathbf{b} \in \mathbb{R}^D$  is drawn from a uniform distribution  $[0, 2\pi]$ . For example, to approximate a Gaussian kernel  $\kappa(\mathbf{x}, \mathbf{x}') = \exp(-\|\mathbf{x} - \mathbf{x}'\|^2 / 2\sigma^2)$ , columns of the frequency matrix  $\boldsymbol{\Omega}$  are i.i.d. sampled from the Gaussian distribution  $\mathcal{N}(0, 1/\sigma^2)$ .

**Remark 14.** For approximate kernel methods (e.g. random Fourier features), the approximate errors have been well-studied in many works [30], [50], [51]. The optimal learning properties of non-parametric regression with random features were proven in [52]. The generalization performance for linear SVM with random features was studied in [53]. These theoretical results illustrate random features provide similar generalization properties as kernel classes. Using random features, our theoretical findings are easily extended to appropriate kernel space.

### 5.4 Mini-batch Gradients for Specific Tasks

In the inequality (15), only the derivative of the loss function  $\frac{\partial \ell(h(\mathbf{x}_i), \mathbf{y}_i)}{\partial \mathbf{W}_t}$  needs to be determined. In this section, we provide this derivative for two specific tasks: multi-class classification and multi-label learning.

Task	Datasets	# training	# testing	# $d$	# $K$
MC	iris	105	45	5	3
	wine	125	53	14	3
	glass	150	64	10	6
	svmguid2	274	117	21	3
	vowel	370	158	11	11
	vehicle	593	253	19	4
	segment	1617	693	19	7
	satimage	3105	1330	37	6
	pendigits	5246	2248	17	10
	letter	10500	4500	17	26
	poker	17507	7503	11	10
	shuttle	27631	11841	10	7
	Sensorless	40957	17552	49	11
	MNIST	42000	18000	718	10
	connect-4	47290	20267	127	3
	acoustic	55177	23646	51	3
covtype	406709	174303	55	7	
MLC	scene	1685	722	295	6
	yeast	1692	725	104	14
	corel5k	3150	1350	500	374
	bibtex	5177	2218	1837	159
MLR	rf2	5376	2303	577	8
	scm1d	6863	2940	281	16

TABLE 4  
Statistics of the experimental datasets.

#### 5.4.1 Multi-class Classification

Consider a multi-class classification problem with  $K$  classes. The output space is written in the one-hot form  $\mathcal{Y} = \{0, 1\}^K$ , which consists of a single 1 and  $K - 1$  zeros.

$$\mathbf{y}_i = [0, \dots, 0, 1, 0, \dots, 0]^T,$$

where only the  $k$ -th element is labeled as one. The margin of multi-class classification is

$$m_h(\mathbf{x}_i, \mathbf{y}_i) = [h(\mathbf{x}_i)]^T \mathbf{y}_i - \max_{\mathbf{y}'_i \neq \mathbf{y}_i} [h(\mathbf{x}_i)]^T \mathbf{y}'_i.$$

The hypothesis  $h$  misclassifies the instance  $(\mathbf{x}_i, \mathbf{y}_i)$  if  $m_h(\mathbf{x}_i, \mathbf{y}_i) \leq 0$ . If 0-1 loss is used, we have  $\ell(h(\mathbf{x}_i), \mathbf{y}_i) = \mathbb{1}_{m_h(\mathbf{x}_i, \mathbf{y}_i) \leq 0}$ . Because the 0-1 loss is not continuous and thus hard to handle, we consider other loss functions that are continuous to upper bound this loss. Specifically, we employ the hinge loss for multi-class classification:

$$\ell(h(\mathbf{x}_i), \mathbf{y}_i) = |1 - m_h(\mathbf{x}_i, \mathbf{y}_i)|_+.$$

The hinge loss is nondifferentiable when  $m_h(\mathbf{x}_i, \mathbf{y}_i) = 0$ , so we use the sub-gradient in this case. For multi-class classification, the sub-gradient of the loss function is

$$\frac{\partial \ell(h(\mathbf{x}_i), \mathbf{y}_i)}{\partial \mathbf{W}_t} = \begin{cases} \mathbf{0}_{D \times K}, & m_h(\mathbf{x}_i, \mathbf{y}_i) \geq 1, \\ \phi(\mathbf{x})[\mathbf{y}'_i - \mathbf{y}_i]^T, & \text{otherwise,} \end{cases} \quad (19)$$

where  $(\mathbf{x}_i, \mathbf{y}_i)$  is an instance from the labeled sample  $\mathcal{D}_l$ .

#### 5.4.2 Multi-label Learning

Consider the multi-label learning scenario with an output space  $\mathcal{Y} = \{0, 1\}^K$  for multi-label classification and  $\mathcal{Y} = \mathbb{R}^K$  for multi-label regression. We define the loss function as  $\ell(h(\mathbf{x}_i), \mathbf{y}_i) = \|\mathbf{y} - h(\mathbf{x}_i)\|_2^2$ . The gradient of the loss is

$$\frac{\partial \ell(h(\mathbf{x}_i), \mathbf{y}_i)}{\partial \mathbf{W}_t} = 2\phi(\mathbf{x}_i)[h(\mathbf{x}_i) - \mathbf{y}_i]^T, \quad (20)$$

where  $(\mathbf{x}_i, \mathbf{y}_i)$  is an instance from the labeled sample  $\mathcal{D}_l$ .

## 6 EXPERIMENTS

We set up four experiments to evaluate the empirical behavior of the proposed algorithm LSVV : (1) average test error of multi-class classification; (2) empirical performance of multi-label learning (test error for multi-label classification and RMSE for multi-label regression); (3) influence of the thresholding  $\theta$ ; (4) influence of the labeled rate.

Parameters	Algorithms
$\tau_I = 0, \tau_S = 0$	SRM-VV [15], [33]
$\tau_I = 0, \tau_S > 0$	LRC-VV [4], [28], [40]
$\tau_I > 0, \tau_S = 0$	SS-VV [54], [55]
$\tau_I > 0, \tau_S > 0$	LSVV

TABLE 5

Compared algorithms for vector-valued output learning.

## 6.1 Experimental Setup

**Datasets.** As demonstrated in Table 4, we use a variety of public benchmark datasets, in which the number of points range from hundreds to hundreds of thousands. These datasets cover two kinds of applications: (1) Multi-class classification (**MC**) with 17 datasets, (2) Multi-label learning, including four datasets for multi-label classification (**MLC**) and two datasets for multi-label regression (**MLR**). To obtain reliable results, we repeat algorithm evaluations 30 times on different dataset partitions of datasets, using 70% of instances as training data and the rest as testing data for each partition.

**Compared Methods.** To verify theoretical findings in the linear space and kernel space, we conduct all algorithms in both two settings: For the linear space, we simply use  $\phi(\mathbf{x}) = \mathbf{x}$  where the feature space is  $\mathcal{S} = \mathbb{R}^d$ ; For the kernel space, as described in Section 5.3, we adopt random Fourier features to approximate kernel hypotheses. To improve scalability of algorithms, only a few random features are used ( $D = 100$ ). As shown in (18), nonlinear feature mappings are used to approximate kernel hypotheses with  $\mathcal{S} = \mathbb{R}^D$  and random features  $\phi(\mathbf{x}) = \sqrt{\frac{2}{D}} \cos(\mathbf{\Omega}^T \mathbf{x} + \mathbf{b})$ .

We compare LSVV to its special cases with various parameter settings for  $\tau_I$  and  $\tau_S$ , listed in Table 5.

- 1) **SRM-VV**: solves the empirical risk minimization with regularization (SRM). This method has been presented for special cases of vector-valued learning, e.g. multi-class [33] and multi-label learning [15].
- 2) **LRC-VV**: solves SRM together with minimizing local Rademacher complexity. It was first proposed for multi-class [28] and for multi-label learning [40].
- 3) **SS-VV**: corresponds to manifold regularization on SRM, which was introduced into multi-class classification [54] and multi-label learning [55].
- 4) **LSVV**: is the proposed algorithm, as shown in (11), which makes use of both local Rademacher complexity and manifold regularization.

**Experimental Settings.** We construct the similarity matrix  $\mathbf{S}$  using a 10-NN graph with binary weights, which are more efficient than the heat kernel weights used in our previous work [29]. The graph Laplacian is given by  $\mathbf{L} = \mathbf{D} - \mathbf{S}$ , where  $\mathbf{D}$  is a diagonal matrix with  $D_{ii} = \sum_{j=1}^{n+u} S_{ij}$ . The predictive ability of LSVV is highly dependent on parameters  $\tau_A, \tau_I, \tau_S$  and the Gaussian kernel parameter  $\sigma$ . For fair comparison, we tune parameters to achieve optimal empirical performance for all algorithms on all datasets, using 5-fold cross-validation and grid search over parameters from candidate sets. The candidate sets consist of the complexity parameter  $\tau_A \in \{10^{-15}, 10^{-14}, \dots, 10^{-6}\}$ , unlabeled samples parameter  $\tau_I \in \{0, 10^{-15}, 10^{-14}, \dots, 10^{-6}\}$ , the parameter for local Rademacher complexity term  $\tau_S \in \{0, 10^{-10}, 10^{-9}, \dots, 10^{-1}\}$ , and tail parameter  $\theta \in \{0, 0.1, \dots, 0.9\} \times \min(K, D)$ . For random Fourier features approaches, the Gaussian kernel parameter  $\sigma$  is selected from the candidate  $[2^{-5}, 2^{-4}, \dots, 2^5]$ .

## 6.2 Evaluations for Multi-class Classification

Compared to our previous work [28], [29], here we conduct experiments on larger datasets with fewer labeled examples. We repeat experiments for compared methods on 17 standard multi-class datasets 30 times, over different partitions (70% as training data and 30% as testing data) each time. In each partition, we uniformly sample 10% of training samples as labeled pairs while the remaining 90% are used as unlabeled instances. Further, the multiple test errors obtained allow the statistical significance of the difference between each method and the optimal result. We adopt a 95% significance level in Table 6, 7. For each dataset, we bold the optimal test error and underline results which show no significant difference from the optimal one.

The results in Table 6 and Table 7 show: (1) Our method outperforms the others on all datasets, both in the linear space and appropriate kernel space. (2) As a classical margin-based multi-class classification model, Linear-VV shows the highest average test errors on all datasets, for both the linear estimator and approximate kernel estimator. This is likely because it does not use local Rademacher complexity and ignores valuable information from unlabeled data. (3) SS-VV makes use of unlabeled instances. LRC-VV minimizes the tail sum of singular values together with the empirical loss and a penalty term for model complexity. SS-VV or LRC-VV only utilize one additional regularizer and obtain comparable performance, being better than Linear-VV but worse than LSVV. (4) Approximate kernel approaches always provide better results than linear approaches. (5) Even using only a small number of random features  $D = 100$ , the results of approximate approaches are significantly better than linear estimators on *iris*, *pendigits*, *shuttle*, *Sensorless* and *MNIST*.

	Linear-VV	SS-VV	LRC-VV	LSVV
iris	29.78±6.21	28.89±4.16	<u>28.44±7.10</u>	<b>28.40±5.53</b>
wine	9.63±3.56	8.89±5.62	<u>6.30±3.10</u>	<b>5.93±4.61</b>
glass	53.54±5.90	51.38±13.61	52.92±3.37	<b>47.69±6.62</b>
svmguid2	39.32±4.30	<u>36.27±8.79</u>	38.98±7.39	<b>35.25±5.45</b>
vowel	74.72±3.28	74.72±3.19	74.72±6.53	<b>69.81±3.42</b>
vehicle	55.43±4.46	54.41±9.40	55.20±6.95	<b>49.45±3.39</b>
segment	17.49±4.79	16.54±2.52	16.62±2.28	<b>14.40±1.61</b>
satimage	21.19±3.47	20.95±1.26	20.78±2.76	<b>19.97±1.41</b>
pendigits	11.85±1.01	11.77±1.42	11.29±1.26	<b>10.30±1.40</b>
letter	48.49±4.88	48.12±2.33	48.22±2.90	<b>44.20±2.90</b>
poker	51.56±3.46	50.67±1.34	51.46±3.55	<b>49.83±0.47</b>
shuttle	6.86±2.00	6.73±1.98	6.19±1.53	<b>5.54±1.77</b>
Sensorless	48.49±4.48	47.08±6.86	47.33±4.28	<b>45.07±2.46</b>
MNIST	17.58±0.25	17.49±0.27	17.52±0.27	<b>17.23±0.34</b>
connect-4	34.18±0.23	34.18±0.22	34.18±0.23	<b>33.73±0.43</b>
acoustic	35.25±1.33	35.18±2.45	<u>34.03±1.25</u>	<b>33.84±1.58</b>
covtype	27.52±2.10	26.44±1.10	26.80±2.93	<b>25.31±1.21</b>

TABLE 6

Comparison of average test error (%) among **linear estimators** for **multi-class classification**.

Datasets	Linear-VV	SS-VV	LRC-VV	LSVV
iris	7.56±5.12	7.56±3.72	7.11±3.65	<b>4.44±3.51</b>
wine	8.15±3.10	<u>6.67±4.83</u>	<u>7.78±4.61</u>	<b>5.56±5.56</b>
glass	44.31±7.80	43.08±6.88	44.31±13.21	<b>37.85±9.27</b>
svmguid2	26.10±2.96	25.93±3.67	25.59±4.77	<b>24.07±2.04</b>
vowel	63.65±2.01	60.13±3.52	63.14±3.23	<b>57.61±3.66</b>
vehicle	45.67±2.43	44.41±4.97	44.80±3.68	<b>41.50±2.31</b>
segment	13.68±1.09	13.56±1.17	13.45±2.18	<b>12.32±1.24</b>
satimage	15.27±0.68	15.16±0.94	15.10±1.84	<b>14.27±0.52</b>
pendigits	6.99±1.07	6.91±0.93	6.95±0.45	<b>6.01±1.27</b>
letter	33.32±0.60	33.14±1.94	33.24±1.82	<b>30.08±1.27</b>
poker	49.94±0.59	49.55±0.68	49.63±0.62	<b>49.19±0.55</b>
shuttle	1.40±0.34	1.26±0.35	1.39±0.26	<b>1.15±0.16</b>
Sensorless	13.31±0.62	13.22±0.25	13.20±0.41	<b>11.55±0.28</b>
MNIST	12.62±0.27	12.57±0.22	<u>12.46±0.47</u>	<b>12.42±0.33</b>
connect-4	30.24±1.23	30.10±1.65	30.02±0.92	<b>29.03±1.25</b>
acoustic	31.45±0.56	31.27±0.41	31.44±0.68	<b>30.23±0.76</b>
covtype	24.24±0.32	24.23±0.26	24.18±0.21	<b>24.09±0.28</b>

TABLE 7

Comparison of average test error (%) among **kernel estimators** for **multi-class classification**.

### 6.3 Evaluations for Multi-label Learning

To study performance on multi-label learning, four multi-label classification tasks and two multi-label regression tasks are utilized. Labels for multi-label classification samples consist of a series of binary classifications. We scale all labels of multi-label regression datasets to  $[0, 1]$ . For multi-label tasks, we consider the case where 50% of labels are missing for training datasets in order to validate the efficiency of the Laplacian regularization. Given a test set  $(\mathbf{x}_i, \mathbf{y}_i)_{i=1}^{n_t}$ , we use the averaged Hamming loss as the criteria to evaluate the generalization performance of multi-label classification:

$$\text{Error} = \frac{1}{n_t K} \sum_{i=1}^{n_t} \sum_{k=1}^K y'_{ik} \oplus y_{ik}.$$

Here,  $y'_i = \mathbf{1}_{h(\mathbf{x}_i) > 0.5}$  and  $\oplus$  is the XOR operator. For the multi-label regression, we employ the averaged root-mean-square error (RMSE):

$$\text{Error} = \frac{1}{n_t K} \sum_{i=1}^{n_t} \|h(\mathbf{x}_i) - \mathbf{y}_i\|_2.$$

Results in Table 8 and Table 9 show that (1) The proposed LSVV with 100 random features always provides the best empirical results among all eight approaches. (2) Both Laplacian regularization (SS-VV) and the tail sum of singular values of  $\mathbf{W}$  (LRC-VV) outperform the structural risk minimization method (Linear-VV) on most datasets.

Dataset	Linear-VV	SS-VV	LRC-VV	LSVV
scene	31.24±4.66	30.98±9.64	16.99±0.50	<b>16.76±0.35</b>
yeast	30.29±3.39	30.08±0.26	27.42±1.92	<b>24.57±1.57</b>
corel5k	28.32±3.29	26.48±3.20	15.14±2.94	<b>1.77±0.50</b>
bibtex	41.72±4.03	41.24±1.52	20.90±43.35	<b>20.89±43.35</b>
rf2	13.42±2.32	12.13±0.87	<u>11.93±0.31</u>	<b>11.93±0.15</b>
scm1d	19.81±12.22	15.39±3.41	18.78±24.00	<b>6.46±3.91</b>

TABLE 8

Comparison of average test error (%) and RMSE among **linear estimators** for **multi-label learning**.

Dataset	Linear-VV	SS-VV	LRC-VV	LSVV
scene	14.99±0.90	14.74±0.41	14.80±0.89	<b>13.46±0.83</b>
yeast	23.05±0.75	22.77±0.39	22.63±0.45	<b>22.32±0.47</b>
corel5k	1.01±0.03	0.98±0.01	0.95±0.02	<b>0.94±0.00</b>
bibtex	1.48±0.01	1.47±0.03	1.45±0.02	<b>1.44±0.04</b>
rf2	1.19±0.09	1.14±0.04	1.03±0.07	<b>0.80±0.05</b>
scm1d	0.68±0.01	0.63±0.03	0.68±0.02	<b>0.53±0.03</b>

TABLE 9

Comparison of average test error (%) and RMSE among **kernel estimators** for **multi-label learning**.

## 6.4 Influence of Labeled Samples

In this section, we focus on improvements brought by manifold regularization, which makes use of unlabeled points. We compare the proposed algorithm  $\text{LSVV}$  with LRC-VV in both the input space and approximate kernel space. Both  $\text{LSVV}$  and LRC-VV make use of SRM and minimize the tail sum of singular values, but  $\text{LSVV}$  also employs unlabeled samples, while LRC-VV only uses labeled data. As shown on the right of Figure 2, the test errors of all methods decrease as the number of labeled samples increases. Meanwhile,  $\text{LSVV}$  outperforms LRC-VV at all label rates.

## 6.5 Influence of the Threshold $\theta$

We vary the thresholding value  $\theta$  for the tail sum of eigenvalues, to determine the importance of an appropriate threshold  $\theta$ . Without a constraint on singular values, if  $\theta = 1$ , the proposed algorithm degrades into the semi-supervised learning approach SS-VV. When  $\theta = 0$ , the tail sum of singular values becomes the trace norm, corresponding to GRC-SS-VV, which bounds the empirical *global* Rademacher complexity. Under the same datasets and settings as in Section 6.3, we compare the proposed algorithm  $\text{LSVV}$  with these two special cases, SS-VV and GRC-SS-VV.

The results are reported in Figure 3. The performance of  $\text{LSVV}$  is limited when  $\theta$  is small.  $\text{LSVV}$  provides the same error rate as GRC-SS-VV when  $\theta = 0$ . However, when  $\theta$  is large, the proposed algorithm obtains comparable performance and will obtain the same error rate as SS-VV. Unlike GRC-SS-VV, there always exists an optimal thresholding  $\theta$  for  $\text{LSVV}$ , offering the lowest error rates. As discussed in Remark 13, an appropriate threshold  $\theta$  is key to obtaining a lower error bound. The empirical results coincide with our theoretical findings (Corollary 9 and Corollary 12).

## 7 PROOF

### 7.1 Proof of Theorem 5

**Proposition 15 (First part of Theorem 3.3 in [35]).** Let  $\mathcal{Z}$  be any set,  $(z_1, \dots, z_m) \in \mathcal{Z}^m$ . For a class of bounded functions  $\mathcal{F} : \mathcal{Z} \rightarrow \mathbb{R}$  with ranges in  $[a, a']$ . Assume there is some function  $T : \mathcal{F} \rightarrow \mathbb{R}^+$  and some constant  $\alpha$  such that for any  $f \in \mathcal{F}$ ,  $\text{Var}(f) \leq T(f) \leq \alpha Pf$ . Assume there is a sub-root function  $\psi$  and a fixed point  $r^*$  of  $\psi$ , for any  $r \geq r^*$  satisfying

$$\psi(r) \geq \alpha \mathcal{R}(\{f \in \mathcal{F} : T(f) \leq r\}). \quad (21)$$

For any  $K > 1$  and any  $\delta \in (0, 1)$ , with a probability of at least  $1 - \delta$ ,

$$Pf \leq \frac{K}{K-1} \hat{P}f + c_1 r^* + c_2 \frac{\log(1/\delta)}{m}, \quad (22)$$

where  $c_1 = \frac{704K}{\alpha}$ ,  $c_2 = 11(a' - a) + 26K\alpha$ ,  $Pf = \mathbb{E}[f(z)]$  is the expectation and  $\hat{P}f = \frac{1}{m} \sum_{i=1}^m f(\mathbf{x}_i)$  is the corresponding empirical version on  $\mathcal{Z}^m$ .

Based on Proposition 15, we prove Theorem 5 as follows.

**Proof of Theorem 5.** According to Proposition 15, we set

$$f = \ell(\hat{h}(\mathbf{x}), \mathbf{y}) - \ell(h^*(\mathbf{x}), \mathbf{y})$$

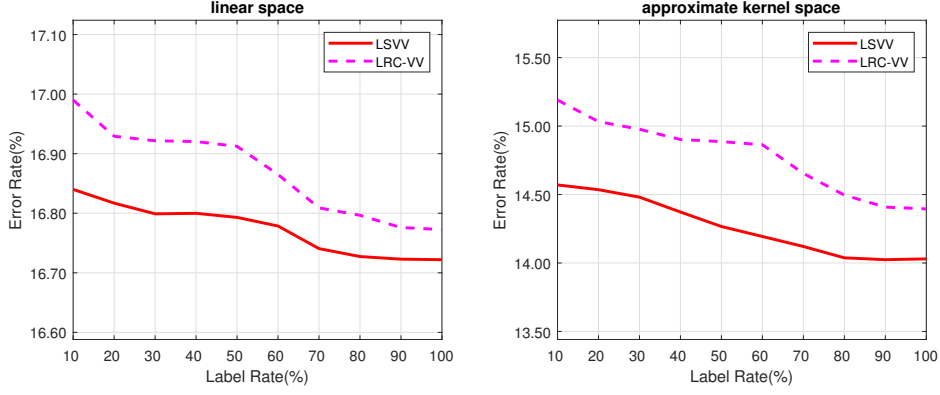
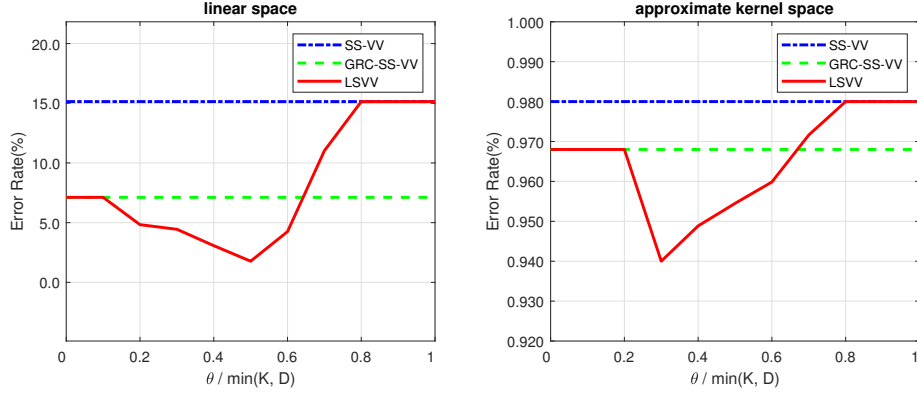
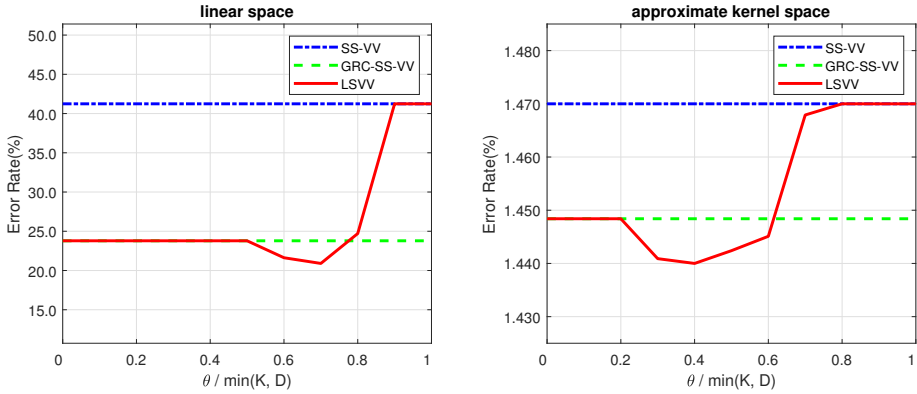


Fig. 2. Empirical performance on *Scene* w.r.t difference label rates.



(a) corel5k



(b) bibtex

Fig. 3. Empirical performance on *corel5k* and *bibtex* w.r.t threshold  $\theta$ .

for any  $(x, y) \in \mathcal{X} \times \mathcal{Y}$ . Here,  $\hat{h} \in \mathcal{H}$  corresponds to the estimator with the minimal empirical loss and  $h^* \in \mathcal{H}$  is the estimator with the minimal expectation loss. Thus, we have  $Pf = \mathcal{E}(\hat{h}) - \mathcal{E}(h^*)$ .

**First step:** (22)  $\rightarrow$  (6). Since  $\hat{h}$  indicates the minimal empirical loss, we have  $\hat{P}f \leq \hat{\mathcal{E}}(\hat{h}) - \hat{\mathcal{E}}(h^*) \leq 0$ . Thus we just omit the  $\hat{P}f$  term in (22) and get

$$\mathcal{E}(\hat{h}) - \mathcal{E}(h^*) \leq c_1 r^* + c_2 \frac{\log(1/\delta)}{n}. \quad (23)$$

Because the loss function  $\ell$  is bounded in  $[0, B]$ , it holds  $f \in [0, B]$ ,  $a' = B$  and  $a = 0$  in Proposition 15. However,  $\mathcal{E}(h^*)$  is also the expected infimum in the loss space, so we have  $Pf = \mathcal{E}(\hat{h}) - \mathcal{E}(h^*) \in [0, B]$ . The variance exists  $\text{Var}(f) = Pf^2 - [Pf]^2 \leq Pf^2 \leq BPf$ . We set  $T(f) = Pf^2$  and then have  $\alpha = B$ . By setting  $\alpha = B$ ,  $a = 0$ ,  $a' = B$  and a small  $K > 1$  in (23), the equation (6) is obtained.

**Second step:** (21)  $\rightarrow$  (5). We consider the variance  $T(f) = Pf^2$ . Thus,  $\mathcal{R}(\{f \in \mathcal{F} : T(f) \leq r\})$  becomes  $\mathcal{R}(\{\mathbb{E}[\ell_{\hat{h}} - \ell_{h^*}]^2 \leq r\})$ , where  $\ell_h = \ell(h(x), y)$  for any  $\ell \in \mathcal{L}$  and  $(x, y) \in \mathcal{X} \times \mathcal{Y}$ , which coincides with local Rademacher complexity

$\mathcal{R}(\mathcal{H}_r)$  in Definition 2. As such (21) requires a sub-root function  $\psi_1$  satisfying

$$\psi_1(r) \geq B\mathcal{R}(\mathcal{L}_r). \quad (24)$$

Using the contraction property in Lemma 4, we have

$$\sqrt{2}BL\mathcal{R}(\mathcal{H}_r) \geq B\mathcal{R}(\mathcal{L}_r). \quad (25)$$

We consider a sub-root function  $\psi(r)$  such that

$$\psi(r) \geq \sqrt{2}BL\mathcal{R}(\mathcal{H}_r). \quad (26)$$

Combining (25) and (26), we then find that the sub-root function  $\psi$  satisfies the condition (24) and we finally get the condition in (5).  $\blacksquare$

## 7.2 Proof of Theorem 7

**Proof of Theorem 7.** Due to the contraction lemma, the symmetry of the  $\epsilon_i$  and  $\|h\|_2 \leq \|h\|_1$ , there exists

$$\begin{aligned} \mathcal{R}(\mathcal{H}_r) &= \mathcal{R}(h \in \mathcal{H}_p : \mathbb{E}[L^2\|h - h^*\|_2^2] \leq r) \\ &= \mathcal{R}(h - h^* : h \in \mathcal{H}_p, \mathbb{E}[\|h - h^*\|_2^2] \leq \frac{r}{L^2}) \\ &\leq \mathcal{R}(h - g : h, g \in \mathcal{H}_p, \mathbb{E}[\|h - g\|_2^2] \leq \frac{r}{L^2}) \\ &= 2\mathcal{R}(h : h \in \mathcal{H}_p, \mathbb{E}[\|h\|_2] \leq \frac{\sqrt{r}}{2L}) \\ &\leq 2\mathcal{R}(h : h \in \mathcal{H}_p, \mathbb{E}[\|h\|_1] \leq \frac{\sqrt{r}}{2L}). \end{aligned}$$

Let  $\|\mathbf{W}\|_p = \|\mathbf{W}\|_{2,1} = \sum_{k=1}^K \|\mathbf{W}_k\|_2$ . We introduce a new hypothesis space  $\mathcal{H}_{2,1}$ , satisfying

$$\mathcal{R}(\mathcal{H}_r) \leq 2\mathcal{R}(\mathcal{H}_{2,1}) \quad (27)$$

where

$$\mathcal{H}_{2,1} = \{\mathbf{x} \rightarrow \mathbf{W}^T \phi(\mathbf{x}) : \|\mathbf{W}\|_{2,1} \leq 1, \mathbb{E}[\|h\|_1] \leq \frac{\sqrt{r}}{2L}\}.$$

For any  $\theta \in \mathbb{N}$ , there holds for local Rademacher complexity

$$\begin{aligned} &\frac{1}{n+u} \sum_{i=1}^{n+u} \sum_{k=1}^K \epsilon_{ik} \langle \mathbf{W}_{\cdot k}, \phi(\mathbf{x}_i) \rangle \\ &= \frac{1}{n+u} \sum_{k=1}^K \left\langle \mathbf{W}, \sum_{i=1}^{n+u} \epsilon_{ik} \phi(\mathbf{x}_i) \right\rangle \\ &= \sum_{k=1}^K \left[ \left\langle \sum_{j=1}^{\theta} \sqrt{\lambda_j} \langle \mathbf{W}_{\cdot k}, \varphi_j \rangle \varphi_j, \sum_{j=1}^{\theta} \frac{1}{\sqrt{\lambda_j}} \left\langle \frac{1}{n+u} \sum_{i=1}^{n+u} \epsilon_{ik} \phi(\mathbf{x}_i), \varphi_j \right\rangle \varphi_j \right\rangle \right. \\ &\quad \left. + \left\langle \mathbf{W}_{\cdot k}, \sum_{j>\theta} \left\langle \frac{1}{n+u} \sum_{i=1}^{n+u} \epsilon_{ik} \phi(\mathbf{x}_i), \varphi_j \right\rangle \varphi_j \right\rangle \right]. \end{aligned} \quad (28)$$

To simplify the presentation, we let

$$\Pi_{jk} = \left\langle \frac{1}{n+u} \sum_{i=1}^{n+u} \epsilon_{ik} \phi(\mathbf{x}_i), \varphi_j \right\rangle. \quad (29)$$

Using (29), the Cauchy-Schwarz inequality and Jensen's inequality, the above inequality (28) yields

$$\begin{aligned} &\mathcal{R}(\mathcal{H}_{2,1}) \\ &= \mathbb{E} \left[ \sup_{h \in \mathcal{H}_{2,1}} \sum_{i=1}^{n+u} \sum_{k=1}^K \epsilon_{ik} \langle \mathbf{W}_{\cdot k}, \phi(\mathbf{x}_i) \rangle \right] \\ &\leq \sup_{h \in \mathcal{H}_{2,1}} \sum_{k=1}^K \sqrt{\left( \sum_{j=1}^{\theta} \lambda_j \langle \mathbf{W}_{\cdot k}, \varphi_j \rangle^2 \right) \left( \sum_{j=1}^{\theta} \frac{1}{\lambda_j} \mathbb{E}[\Pi_{jk}^2] \right)} + \sum_{k=1}^K \|\mathbf{W}_{\cdot k}\|_2 \sqrt{\sum_{j>\theta} \mathbb{E}[\Pi_{jk}^2]}. \end{aligned} \quad (30)$$



By the eigenvalue decomposition, it holds that  $\mathbb{E}[\|h_y\|] = \sqrt{\sum_{j=1}^{\infty} \lambda_j \langle \mathbf{W} \cdot_k, \varphi_j \rangle^2}$ , such that

$$\sum_{k=1}^K \sqrt{\sum_{j=1}^{\theta} \lambda_j \langle \mathbf{W} \cdot_k, \varphi_j \rangle^2} \leq \mathbb{E}[\|h\|_1] \leq \frac{\sqrt{r}}{2L}. \quad (31)$$

Substituting (31) and  $\|\mathbf{W}\|_{2,1} \leq 1$  into (30), we obtain

$$\mathcal{R}(\mathcal{H}_{2,1}) \leq \min_{0 \leq \theta \leq n+u} \frac{\sqrt{r}}{2L} \sqrt{\sum_{j=1}^{\theta} \frac{1}{\lambda_j} \mathbb{E}_{\epsilon}[\Pi_{jk}^2]} + \sqrt{\sum_{j>\theta} \mathbb{E}_{\epsilon}[\Pi_{jk}^2]}. \quad (32)$$

Moreover, we define  $\widehat{C}$  as the corresponding operator of  $\mathbf{K}$  and apply the symmetry of Rademacher variables

$$\begin{aligned} & \mathbb{E}_{\epsilon}[\Pi_{jk}^2] \\ &= \frac{1}{(n+u)^2} \mathbb{E}_{\epsilon} \sum_{i,l=1}^{n+u} \epsilon_{ik} \epsilon_{lk} \langle \phi(\mathbf{x}_i), \varphi_j \rangle \langle \phi(\mathbf{x}_l), \varphi_j \rangle \\ &= \frac{1}{(n+u)^2} \sum_{i=1}^{n+u} \langle \phi(\mathbf{x}_i), \varphi_j \rangle^2 \\ &= \frac{1}{n+u} \langle \varphi_j, \widehat{C} \varphi_j \rangle \\ &= \frac{\lambda_j}{n+u}. \end{aligned} \quad (33)$$

Substituting (32) and (33) into (27), we have

$$\mathcal{R}(\mathcal{H}_r) \leq 2\mathcal{R}(\mathcal{H}_{2,1}) \leq \min_{0 \leq \theta \leq n+u} \frac{1}{L} \sqrt{\frac{\theta r}{n+u}} + 2 \sqrt{\sum_{j=\theta+1}^{n+u} \frac{\lambda_j}{n+u}}. \quad (34)$$

Applying these results, we complete the proof. ■

### 7.3 Proof of Theorem 10

**Proof of Theorem 10.** Due to the contraction lemma, the symmetry of Rademacher variables and  $\mathbb{E}[\mathbf{x}^T \mathbf{x}] \leq 1$ , we have

$$\begin{aligned} \mathcal{R}(\mathcal{H}_r) &= \mathcal{R}(h \in \mathcal{H}_p : \mathbb{E}[L^2 \|h - h^*\|_2^2] \leq r) \\ &= \mathcal{R}(h - h^* : h \in \mathcal{H}_p, \mathbb{E}[\|h - h^*\|_2^2] \leq \frac{r}{L^2}) \\ &\leq \mathcal{R}(h - g : h, g \in \mathcal{H}_p, \mathbb{E}[\|h - g\|_2^2] \leq \frac{r}{L^2}) \\ &= 2\mathcal{R}(h : h \in \mathcal{H}_p, \mathbb{E}[\|h\|_2^2] \leq \frac{r}{4L^2}) \\ &= 2\mathcal{R}(h : h \in \mathcal{H}_p, \mathbb{E}[\mathbf{x}^T \mathbf{W} \mathbf{W}^T \mathbf{x}] \leq \frac{r}{4L^2}) \\ &= 2\mathcal{R}(h : h \in \mathcal{H}_p, \mathbb{E}[\|\mathbf{W} \mathbf{W}^T\|] \leq \frac{\sqrt{r}}{2L}) \\ &= 2\mathcal{R}(\mathcal{H}_r^{\mathbf{W}}). \end{aligned} \quad (35)$$

The inequalities above provide a constraint on  $\mathbf{W}$  that is  $\mathbb{E}[\|\mathbf{W} \mathbf{W}^T\|] \leq \frac{\sqrt{r}}{2L}$ , which is useful when we reduce terms related to  $\mathbf{W}$ . Then, local Rademacher complexity  $\mathcal{R}(\mathcal{H}_r^{\mathbf{W}})$  can be rewritten as

$$\begin{aligned} \mathcal{R}(\mathcal{H}_r^{\mathbf{W}}) &= \mathbb{E} \left[ \sup_{h \in \mathcal{H}_r^{\mathbf{W}}} \frac{1}{n+u} \sum_{i=1}^{n+u} \sum_{k=1}^K \epsilon_{ik} h_j(\mathbf{x}_i) \right] \\ &= \mathbb{E} \left[ \sup_{h \in \mathcal{H}_r^{\mathbf{W}}} \frac{1}{n+u} \sum_{i=1}^{n+u} \sum_{k=1}^K \epsilon_{ik} \mathbf{W}_{\cdot j}^T \phi(\mathbf{x}_i) \right] \\ &= \mathbb{E} \left[ \sup_{h \in \mathcal{H}_r^{\mathbf{W}}} \sum_{k=1}^K \mathbf{W}_{\cdot j}^T \left( \frac{1}{n+u} \sum_{i=1}^{n+u} \epsilon_{ik} \phi(\mathbf{x}_i) \right) \right] \\ &= \mathbb{E} \left[ \sup_{h \in \mathcal{H}_r^{\mathbf{W}}} \langle \mathbf{W}, \mathbf{X}_{\epsilon} \rangle \right], \end{aligned} \quad (36)$$

where  $\mathbf{W}, \mathbf{X}_\epsilon \in \mathbb{R}^{D \times K}$  and  $\langle \mathbf{W}, \mathbf{X}_\epsilon \rangle = \text{Tr}(\mathbf{W}^T \mathbf{X}_\epsilon)$  represents the trace norm. We define the matrix  $\mathbf{X}_\epsilon$  as follows:

$$\mathbf{X}_\epsilon := \left[ \frac{1}{n+u} \sum_{i=1}^{n+u} \epsilon_{i1} \phi(\mathbf{x}_i), \dots, \frac{1}{n+u} \sum_{i=1}^{n+u} \epsilon_{iK} \phi(\mathbf{x}_i) \right].$$

More interesting details of the trace norm can be found in [56]. Borrowing the proof sketches of Theorem 5 in [40], we consider the SVD decomposition

$$\mathbf{W} = \sum_{j \geq 1} \mathbf{u}_j \mathbf{v}_j^T \tilde{\lambda}_j,$$

where  $\mathbf{u}_j$  and  $\mathbf{v}_j$  are the orthogonal vectors. It holds the following inequalities

$$\begin{aligned} \langle \mathbf{W}, \mathbf{X}_\epsilon \rangle &\leq \sum_{j=1}^{\theta} \langle \mathbf{u}_j \mathbf{v}_j^T \tilde{\lambda}_j, \mathbf{X}_\epsilon \mathbf{u}_j \mathbf{u}_j^T \rangle + \sum_{j>\theta} \langle \mathbf{W}, \mathbf{X}_\epsilon \mathbf{u}_j \mathbf{u}_j^T \rangle \\ &\leq \left\langle \sum_{j=1}^{\theta} \mathbf{u}_j \mathbf{v}_j^T \tilde{\lambda}_j, \sum_{j=1}^{\theta} \mathbf{X}_\epsilon \mathbf{u}_j \mathbf{u}_j^T \right\rangle + \left\langle \mathbf{W}, \sum_{j>\theta} \mathbf{X}_\epsilon \mathbf{u}_j \mathbf{u}_j^T \right\rangle \\ &\leq \left\| \sum_{j=1}^{\theta} \mathbf{u}_j \mathbf{v}_j^T \tilde{\lambda}_j \right\| \left\| \sum_{j=1}^{\theta} \mathbf{X}_\epsilon \mathbf{u}_j \mathbf{u}_j^T \tilde{\lambda}_j^{-1} \right\| + \|\mathbf{W}\|_* \left\| \sum_{j>\theta} \mathbf{X}_\epsilon \mathbf{u}_j \mathbf{u}_j^T \right\|. \end{aligned}$$

Then, we begin to bound the norm terms in the above inequalities. According to the definition of  $\mathcal{H}_r^{\mathbf{W}}$ , it holds that  $\mathbb{E}[\|\mathbf{W}\mathbf{W}^T\|] \leq \frac{\sqrt{r}}{2L}$ . Thus, we have

$$\left\| \sum_{j=1}^{\theta} \mathbf{u}_j \mathbf{v}_j^T \tilde{\lambda}_j \right\| = \left\| \sum_{j=1}^{\theta} \mathbf{u}_j \mathbf{u}_j^T \tilde{\lambda}_j \right\| \leq \left\| \sum_{j=1}^{\infty} \mathbf{u}_j \mathbf{u}_j^T \tilde{\lambda}_j \right\| = \|\mathbb{E}[\mathbf{W}\mathbf{W}^T]\| \leq \frac{\sqrt{r}}{2L}. \quad (37)$$

Using the properties of SVD decomposition, there exists

$$\mathbb{E} \left[ \left\| \sum_{j=1}^{\theta} \mathbf{X}_\epsilon \mathbf{u}_j \mathbf{u}_j^T \tilde{\lambda}_j^{-1} \right\| \right] = \mathbb{E} \left[ \sqrt{\sum_{j=1}^{\theta} \tilde{\lambda}_j^{-2} \langle \mathbf{X}_\epsilon, \mathbf{u}_j \rangle^2} \right] \leq \sqrt{\sum_{j=1}^{\theta} \frac{\tilde{\lambda}_j^{-2}}{n+u} \mathbb{E}[\langle \phi(\mathbf{x}), \mathbf{u}_j \rangle^2]} \leq \sqrt{\frac{\theta}{n+u}}. \quad (38)$$

Then, we also have

$$\mathbb{E} \left[ \left\| \sum_{j>\theta} \mathbf{X}_\epsilon \mathbf{u}_j \mathbf{u}_j^T \right\| \right] \leq \sqrt{\frac{1}{n+u} \sum_{j>\theta} \tilde{\lambda}_j^2}. \quad (39)$$

We set the norm of  $\|\mathbf{W}\|_p$  in  $\mathcal{H}_r^{\mathbf{W}}$  as trace norm

$$\|\mathbf{W}\|_* \leq 1. \quad (40)$$

Substituting (37), (38), (39) and (40) into (36), we then have

$$\mathcal{R}(\mathcal{H}_r^{\mathbf{W}}) = \mathbb{E} \left[ \sup_{h \in \mathcal{H}_r^{\mathbf{W}}} \langle \mathbf{W}, \mathbf{X}_\epsilon \rangle \right] \leq \min_{0 \leq \theta} \frac{1}{2L} \sqrt{\frac{\theta r}{n+u}} + \sqrt{\frac{1}{n+u} \sum_{j>\theta} \tilde{\lambda}_j^2}. \quad (41)$$

Combining (35) and (41), we have

$$\mathcal{R}(\mathcal{H}_r) \leq 2\mathcal{R}(\mathcal{H}_r^{\mathbf{W}}) \leq \min_{0 \leq \theta} \frac{1}{L} \sqrt{\frac{\theta r}{n+u}} + 2 \sqrt{\sum_{j=\theta+1}^{n+u} \frac{\tilde{\lambda}_j^2}{n+u}}. \quad (42)$$

We complete the proof. ■

## 7.4 Partly Singular Values Thresholding

In each iteration, to obtain a tight surrogate of Eq. (11), we keep  $\tau_S \sum_{j>\theta} \lambda_j(\mathbf{W})$  while only relaxing  $g(\mathbf{W})$ , leading to a proximal regularization of  $g(\mathbf{W})$  at  $\mathbf{W}_t$

$$\begin{aligned} \mathbf{W}_{t+1} &= \arg \min_{\mathbf{W}} g(\mathbf{W}_t) + \langle \nabla g(\mathbf{W}_t), \mathbf{W} - \mathbf{W}_t \rangle + \frac{1}{2\eta_t} \|\mathbf{W} - \mathbf{W}_t\|_F^2 + \tau_S \sum_{j>\theta} \lambda_j(\mathbf{W}) \\ &= \arg \min_{\mathbf{W}} \frac{1}{2\eta_t} \|\mathbf{W} - (\mathbf{W}_t - \eta_t \nabla g(\mathbf{W}_t))\|_F^2 + \tau_S \sum_{j>\theta} \lambda_j(\mathbf{W}), \end{aligned} \quad (43)$$

where  $\eta_t$  is the learning rate at the  $t$ -th iteration to update gradients,  $\nabla g(\mathbf{W}_t)$  is the derivative of  $g(\mathbf{W})$  at  $\mathbf{W}_t$  and terms independent on  $\mathbf{W}$  are ignored.

**Proposition 16 (Theorem 6 of [40]).** Let  $\mathbf{Q}_t \in \mathbb{R}^{D \times K}$  with rank  $r$ . Its SVD decomposition is  $\mathbf{Q}_t = \mathbf{U} \mathbf{\Sigma} \mathbf{V}^T$ , where  $\mathbf{U} \in \mathbb{R}^{D \times r}$  and  $\mathbf{V} \in \mathbb{R}^{K \times r}$  have orthogonal columns and  $\mathbf{\Sigma}$  is diagonal. Then, it holds

$$\mathcal{D}_\tau^\theta(\mathbf{Q}_t) = \arg \min_{\mathbf{W}} \left\{ \frac{1}{2} \|\mathbf{W} - \mathbf{Q}_t\|_F^2 + \tau \sum_{j>\theta} \lambda_j(\mathbf{W}) \right\}, \quad (44)$$

is given by  $\mathcal{D}_\tau^\theta = \mathbf{U} \mathbf{\Sigma}_\tau^\theta \mathbf{V}^T$ , where  $\mathbf{\Sigma}_\tau^\theta$  is diagonal with

$$(\mathbf{\Sigma}_\tau^\theta)_{jj} = \begin{cases} |\Sigma_{jj} - \tau|_+ & j \leq \theta, \\ \Sigma_{jj}, & j > \theta. \end{cases}$$

Applied to Proposition 16, the proximal mapping (43) is equal to (44) with  $\tau = \eta_t \tau_S$ , and then we get the result.

## 8 CONCLUSION

Based on our previous works for multi-class classification [28], [29], we introduce local Rademacher complexity for vector-valued learning with unlabeled samples. Firstly, using the notion of local Rademacher complexity and unlabeled data, we study the generalization properties of vector-valued functions and present much tighter generalization error bounds for both linear hypotheses and kernel hypotheses. Motivated by our statistical analysis, we devise a unified learning framework based on generic empirical risk minimization (ERM), adding the manifold regularization term to use unlabeled data and the tail sum of singular values term to bound local Rademacher complexity. Extensive empirical results on a wide range of benchmark datasets show that our learning framework offers great improvements for vector-valued tasks, which corroborates our theoretical findings.

## REFERENCES

- [1] J. C. Platt, N. Cristianini, and J. Shawe-Taylor, "Large margin dags for multiclass classification," in *Advances in Neural Information Processing Systems 13 (NIPS)*, 2000, pp. 547–553.
- [2] C. Cortes, M. Mohri, and A. Rostamizadeh, "Multi-class classification with maximum margin multiple kernel," in *Proceedings of the 30th International Conference on Machine Learning (ICML)*, 2013, pp. 46–54.
- [3] M.-L. Zhang and Z.-H. Zhou, "A review on multi-label learning algorithms," *IEEE transactions on knowledge and data engineering*, vol. 26, no. 8, pp. 1819–1837, 2013.
- [4] H.-F. Yu, P. Jain, P. Kar, and I. Dhillon, "Large-scale multi-label learning with missing labels," in *Proceedings of the 31st International Conference on Machine Learning (ICML)*, 2014, pp. 593–601.
- [5] Y. Zhang and Q. Yang, "A survey on multi-task learning," *arXiv preprint arXiv:1707.08114*, 2017.
- [6] W. Wang, Y. Liang, and E. P. Xing, "Collective support recovery for multi-design multi-response linear regression," *IEEE Transactions on Information Theory*, vol. 61, no. 1, pp. 513–534, 2014.
- [7] Z. Wang, Z. Zhu, and D. Li, "Collaborative and geometric multi-kernel learning for multi-class classification," *Pattern Recognition*, vol. 99, p. 107050, 2020.
- [8] D. Cireřan, U. Meier, and J. Schmidhuber, "Multi-column deep neural networks for image classification," *arXiv preprint arXiv:1202.2745*, 2012.
- [9] L. Li, H. He, and J. Li, "Entropy-based sampling approaches for multi-class imbalanced problems," *IEEE Transactions on Knowledge and Data Engineering*, vol. 32, no. 11, pp. 2159–2170, 2019.
- [10] E. R. Fernandes, A. C. de Carvalho, and X. Yao, "Ensemble of classifiers based on multiobjective genetic sampling for imbalanced data," *IEEE Transactions on Knowledge and Data Engineering*, vol. 32, no. 6, pp. 1104–1115, 2019.
- [11] J. Zhang, Y. Wang, Y. Sun, and G. Li, "Strength of ensemble learning in multiclass classification of rockburst intensity," *International Journal for Numerical and Analytical Methods in Geomechanics*, vol. 44, no. 13, pp. 1833–1853, 2020.
- [12] M. Xu, Y.-F. Li, and Z.-H. Zhou, "Multi-label learning with pro loss," in *Proceedings of the 27th AAAI Conference on Artificial Intelligence (AAAI)*, 2013.
- [13] M.-L. Zhang and Z.-H. Zhou, "MI-knn: A lazy learning approach to multi-label learning," *Pattern recognition*, vol. 40, no. 7, pp. 2038–2048, 2007.
- [14] N. Rastin, M. Z. Jahromi, and M. Taheri, "A generalized weighted distance k-nearest neighbor for multi-label problems," *Pattern Recognition*, vol. 114, p. 107526, 2021.
- [15] S. Ji, L. Sun, R. Jin, and J. Ye, "Multi-label multiple kernel learning," in *Advances in neural information processing systems*, 2009, pp. 777–784.
- [16] L. Wang, Y. Liu, C. Qin, G. Sun, and Y. Fu, "Dual relation semi-supervised multi-label learning," in *Proceedings of the AAAI Conference on Artificial Intelligence*, vol. 34, no. 04, 2020, pp. 6227–6234.
- [17] N. Xu, Y.-P. Liu, and X. Geng, "Partial multi-label learning with label distribution," in *Proceedings of the AAAI Conference on Artificial Intelligence*, vol. 34, no. 04, 2020, pp. 6510–6517.

- [18] M.-K. Xie and S.-J. Huang, "Partial multi-label learning with noisy label identification," *IEEE Transactions on Pattern Analysis and Machine Intelligence*, 2021.
- [19] C. A. Micchelli and M. Pontil, "On learning vector-valued functions," *Neural computation*, vol. 17, no. 1, pp. 177–204, 2005.
- [20] C. Carmeli, E. De Vito, A. Toigo, and V. Umanitá, "Vector valued reproducing kernel hilbert spaces and universality," *Analysis and Applications*, vol. 8, no. 01, pp. 19–61, 2010.
- [21] M. H. Quang, L. Bazzani, and V. Murino, "A unifying framework for vector-valued manifold regularization and multi-view learning," in *International Conference on Machine Learning*, 2013, pp. 100–108.
- [22] V. Koltchinskii, "Rademacher penalties and structural risk minimization," *IEEE Transactions on Information Theory*, vol. 47, no. 5, pp. 1902–1914, 2001.
- [23] P. L. Bartlett and S. Mendelson, "Rademacher and gaussian complexities: Risk bounds and structural results," *Journal of Machine Learning Research*, vol. 3, no. Nov, pp. 463–482, 2002.
- [24] Y. Lei, U. Dogan, A. Binder, and M. Kloft, "Multi-class SVMs: From tighter data-dependent generalization bounds to novel algorithms," in *Advances in Neural Information Processing Systems 28 (NIPS)*, 2015, pp. 2035–2043.
- [25] C. Cortes, V. Kuznetsov, M. Mohri, and S. Yang, "Structured prediction theory based on factor graph complexity," in *Advances in Neural Information Processing Systems 29 (NIPS)*, 2016, pp. 2514–2522.
- [26] A. Maurer, "A vector-contraction inequality for rademacher complexities," in *International Conference on Algorithmic Learning Theory*. Springer, 2016, pp. 3–17.
- [27] L. Wu, A. Ledent, Y. Lei, and M. Kloft, "Fine-grained generalization analysis of vector-valued learning," in *Proceedings of the AAAI Conference on Artificial Intelligence*, vol. 35, no. 12, 2021, pp. 10338–10346.
- [28] J. Li, Y. Liu, R. Yin, H. Zhang, L. Ding, and W. Wang, "Multi-class learning: From theory to algorithm," in *Advances in Neural Information Processing Systems 31 (NeurIPS)*, 2018, pp. 1591–1600.
- [29] J. Li, Y. Liu, R. Yin, and W. Wang, "Multi-class learning using unlabeled samples : Theory and algorithm," in *Proceedings of the 28th International Joint Conference on Artificial Intelligence (IJCAI)*, 2019.
- [30] A. Rahimi and B. Recht, "Random features for large-scale kernel machines," in *Advances in Neural Information Processing Systems 21 (NIPS)*, 2007, pp. 1177–1184.
- [31] E. L. Allwein, R. E. Schapire, and Y. Singer, "Reducing multiclass to binary: A unifying approach for margin classifiers," *Journal of Machine Learning Research*, vol. 1, pp. 113–141, 2000.
- [32] A. Daniely, S. Sabato, S. Ben-David, and S. Shalev-Shwartz, "Multiclass learnability and the erm principle," *Journal of Machine Learning Research*, vol. 16, no. 1, pp. 2377–2404, 2015.
- [33] V. Koltchinskii, D. Panchenko, and F. Lozano, "Some new bounds on the generalization error of combined classifiers," in *Advances in Neural Information Processing Systems 14 (NIPS)*, 2001, pp. 245–251.
- [34] Y. Maximov and D. Reshetova, "Tight risk bounds for multi-class margin classifiers," *Pattern Recognition and Image Analysis*, vol. 26, no. 4, pp. 673–680, 2016.
- [35] P. L. Bartlett, O. Bousquet, S. Mendelson *et al.*, "Local rademacher complexities," *The Annals of Statistics*, vol. 33, no. 4, pp. 1497–1537, 2005.
- [36] Y. Wei, F. Yang, and M. J. Wainwright, "Early stopping for kernel boosting algorithms: A general analysis with localized complexities," *IEEE Transactions on Information Theory*, vol. 65, no. 10, pp. 6685–6703, 2019.
- [37] Y. Maximov, M.-R. Amini, and Z. Harchaoui, "Rademacher complexity bounds for a penalized multi-class semi-supervised algorithm," *Journal of Artificial Intelligence Research*, vol. 61, pp. 761–786, 2018.
- [38] F. Abramovich, V. Grinshtein, and T. Levy, "Multiclass classification by sparse multinomial logistic regression," *IEEE Transactions on Information Theory*, 2021.
- [39] J. R. Doppa, J. Yu, C. Ma, A. Fern, and P. Tadepalli, "Hc-search for multi-label prediction: An empirical study," in *Proceedings of the 28th AAAI Conference on Artificial Intelligence (AAAI)*, 2014.
- [40] C. Xu, T. Liu, D. Tao, and C. Xu, "Local rademacher complexity for multi-label learning," *IEEE Transactions on Image Processing*, vol. 25, no. 3, pp. 1495–1507, 2016.
- [41] B. Schölkopf and A. J. Smola, *Learning with kernels*. Cambridge, MA: MIT Press, 2002.
- [42] C. Cortes, M. Kloft, and M. Mohri, "Learning kernels using local rademacher complexity," in *Advances in Neural Information Processing Systems 26 (NIPS)*, 2013, pp. 2760–2768.
- [43] Y. Lei, Ü. Dogan, D.-X. Zhou, and M. Kloft, "Data-dependent generalization bounds for multi-class classification," *IEEE Transactions on Information Theory*, vol. 65, no. 5, pp. 2995–3021, 2019.
- [44] V. Koltchinskii and D. Panchenko, "Empirical margin distributions and bounding the generalization error of combined classifiers," *The Annals of Statistics*, vol. 30, pp. 1–50, 2002.
- [45] N. Srebro, K. Sridharan, and A. Tewari, "Smoothness, low noise and fast rates," in *Advances in Neural Information Processing Systems 22 (NIPS)*, 2010, pp. 2199–2207.
- [46] R. Johnson and T. Zhang, "Graph-based semi-supervised learning and spectral kernel design," *IEEE Transactions on Information Theory*, vol. 54, no. 1, pp. 275–288, 2008.
- [47] W. Liu and S.-F. Chang, "Robust multi-class transductive learning with graphs," in *Proceedings of the 22nd IEEE Conference on Computer Vision and Pattern Recognition (CVPR)*. IEEE, 2009, pp. 381–388.
- [48] W. Liu, J. He, and S.-F. Chang, "Large graph construction for scalable semi-supervised learning," in *Proceedings of the 27th International Conference on Machine Learning (ICML)*, 2010, pp. 679–686.
- [49] A. Anis, A. El Gamal, A. S. Avestimehr, and A. Ortega, "A sampling theory perspective of graph-based semi-supervised learning," *IEEE Transactions on Information Theory*, vol. 65, no. 4, pp. 2322–2342, 2019.
- [50] Q. Le, T. Sarló, and A. Smola, "Fastfood-approximating kernel expansions in loglinear time," in *Proceedings of the 30th International Conference on Machine Learning (ICML)*, vol. 85, 2013.
- [51] F. X. X. Yu, A. T. Suresh, K. M. Choromanski, D. N. Holtmann-Rice, and S. Kumar, "Orthogonal random features," in *Advances in Neural Information Processing Systems 29 (NIPS)*, 2016, pp. 1975–1983.
- [52] A. Rudi and L. Rosasco, "Generalization properties of learning with random features," in *Advances in Neural Information Processing Systems 30 (NIPS)*, 2017, pp. 3215–3225.
- [53] Y. Sun, A. Gilbert, and A. Tewari, "But how does it work in theory? linear svm with random features," in *Advances in Neural Information Processing Systems*, 2018, pp. 3379–3388.
- [54] X. Li, Y. Guo, and D. Schuurmans, "Semi-supervised zero-shot classification with label representation learning," in *Proceedings of the IEEE International Conference on Computer Vision (ICCV)*, 2015, pp. 4211–4219.
- [55] Y. Luo, D. Tao, B. Geng, C. Xu, and S. J. Maybank, "Manifold regularized multitask learning for semi-supervised multilabel image classification," *IEEE Transactions on Image Processing*, vol. 22, no. 2, pp. 523–536, 2012.
- [56] S. M. Kakade, S. Shalev-Shwartz, and A. Tewari, "Regularization techniques for learning with matrices," *Journal of Machine Learning Research*, vol. 13, no. Jun, pp. 1865–1890, 2012.